Turkish Journal of Earth Sciences (Turkish J. Earth Sci.), Vol. 21, 2012, pp. 289–314. Copyright ©TÜBİTAK
doi:10.3906/yer-1005-3 First published online 16 December 2010

Variability of Neogene Continental Climates in Northwest Europe – A Detailed Study Based on Microfloras

TORSTEN UTESCHER[1], ABDUL R. ASHRAF[2], ANDREAS DREIST[1], KAREN DYBKJÆR[3], VOLKER MOSBRUGGER[4], JÖRG PROSS[5] & VOLKER WILDE[4]

[1] Steinmann Institute, Bonn University, 53115 Bonn, Germany
(E-mail: utescher@geo.uni-bonn.de)
[2] Institute for Geosciences, Eberhard Karls University, 72076 Tübingen, Germany
[3] Geological Survey of Denmark and Greenland, 1350 Copenhagen K, Denmark
[4] Senckenberg Research Institute and Natural History Museum, 60325 Frankfurt, Germany
[5] Paleoenvironmental Dynamics Group, Institute of Geosciences, Goethe University, 60438 Frankfurt, Germany

Received 07 May 2010; revised typescripts received 16 August 2010 & 26 November 2010; accepted 16 December 2011

Abstract: This study presents a detailed continental palaeoclimate record for the Neogene of Northwestern Europe. Palynomorph samples from continental to marginal marine deposits in 5 correlated sections from the Lower Rhine Basin (NW Germany) covering the time-span from Burdigalian to Zanclean are analysed. Independent time-control in the sections is provided by sequence stratigraphy. Based on 1470 microfloras 3 temperature (mean annual temperature, warm and cold month mean) and 4 precipitation variables (mean annual precipitation, mean monthly precipitation in the driest, wettest and warmest month) are quantified using the Coexistence Approach, a method employing climate requirements of Nearest Living Relatives of fossil taxa.

In face of known limitations in climatic resolution of microflora-based data, present results confirm the major trends in continental Neogene climate evolution of Northwestern Europe as previously reconstructed from macroflora and, in addition, reveal climate change on shorter time scales. Our data suggest a distinct coupling of continental climate with the marine environmental system. Phases of eustatic sea-level lowstand connected to Neogene glaciation events (Mi events) are mirrored in the continental curves. The continental records also show cyclicity at different scales and amplitudes. Small-scale climate variability we observe in the Mid-Miocene and the Tortonian most probably is paced by eccentricity (100 kyr cycles), in the later part of the Langhian and early Serravallian 400 kyr cycles are expressed as well. Along the time-span regarded climate variability is characterized by non-proportional changes of climate variables. During the Miocene, cooling – mainly expressed by a decrease in winter temperature – commonly was connected to drying. A substantial shift of the climate system is indicated for the Pliocene where warm periods tended to be summer-dry, at the same time higher amplitudes of short-term changes point to decreasing climate stability.

Key Words: Neogene, continental palaeoclimate, orbital cycles, palynomorphs, climate variability, Northwest Germany, Lower Rhine Basin

Kuzeybatı Avrupa Neojen Karasal İklimlerinin Değişimi – Mikrofloralara Dayalı Ayrıntılı Bir Çalışma

Özet: Bu çalışmada, Kuzeybatı Avrupa'nın Neojen'inden ayrıntılı bir karasal paleoiklimsel kayıt sunulmaktadır. Burdigaliyen'den Zankleyan'a kadar olan zaman aralığı içinde, Alt Rhine Havzası'ndan (KB Almanya) karasal ve deniz kıyısı çökellerini içeren karşılaştırılmış 5 kesitten alınmış palinomorf örnekleri analiz edilmiştir. Bu kesitlerdeki bağımsız zaman kontrolü sekans stratigrafisi ile sağlanmıştır. 1470 mikroflorayı temel alan, 3 sıcaklık (yıllık ortalama sıcaklık değeri, sıcak ve soğuk ayların ortalaması) ve 4 yağış değişkenleri (yıllık ortalama yağış miktarı, en kurak, en nemli ve en ılık aylara ait ortalama yağış miktarları) fosil taksaların yaşayan en yakın akrabalarının iklimsel gereksinimlerini temel alan Birarada Olma Yaklaşımı yöntemi ile hesaplanmıştır.

Ayrıca, mevcut sonuçlardaki mikrofloraya dayalı verilerin iklimsel çözünürlüklerindeki bilinen sınırlamalar, daha önce makrofloralardan yeniden düzenlendiği gibi Kuzeybatı Avrupa'nın karasal Neojen iklimsel evrimindeki temel gidişleri doğrulamaktadır ve daha kısa zaman cetvellerindeki iklimsel değişimi açığa çıkarmaktadır. Bulgularımız, denizel ortam sistemi ile karasal iklimin belirgin bir bağlantısı olduğu fikrini vermektedir. Neojen buzullaşma olaylarıyla bağlantılı (Mi olayları) östatik en düşük deniz seviyesi fazları karasal eğriler üzerine yansıtılmıştır. Karasal kayıtlar da, farklı ölçeklerde ve büyüklüklerde devirsellik göstermektedir. Orta Miyosen ve Tortoniyen'de gözlediğimiz küçük ölçekteki iklimsel değişim, büyük olasılıkla eksantriklik tarafından (100 kyr döngüleri) düzene girer, Langiyen'in ve erken Serravaliyen'in daha sonraki bölümünde 400 kyr döngüleri olarak da ifade edilmiştir. Zaman aralığı boyunca kabul edilen iklimsel değişim, iklimsel değişimlerin oransal olmayan değişiklikleri ile tanımlanmıştır. Miyosen süresince, kış sıcaklığındaki bir düşüşle ifade edilen soğuma genellikle kuraklığa bağlanmıştır. İklim sistemindeki önemli bir değişim, ılık dönemlerin yaz kuraklığı eğiliminde olduğu ve aynı zamanda kısa süreli değişimlerin daha yüksek büyüklüklerde azalan iklim duraylılığına işaret ettiği Pliyosen için gösterilmiştir.

Anahtar Sözcükler: Neojen, karasal paleoiklim, yörünge döngüleri, palinomorflar, iklim değişimi, Kuzeybatı Almanya, Alt Rhine Havzası

Introduction

Comprehensive studies exist on marine evidence for the global climate evolution during the Cenozoic, and for climate variability at different time scales using a variety of proxy data and methods (e.g., Miller *et al.* 1998, 2005; Zachos *et al.* 2001, 2008; Holbourn *et al.* 2005; Westerhold *et al.* 2005). The study of stable-isotope chemistry unravels changes in ocean water temperatures and global ice volume, and provides insights into ocean circulation patterns and into the carbon cycle, while sedimentological data provide information on runoff and weathering on the continents. However, marine proxies commonly do not offer the possibility for reconstructing palaeoclimatic conditions for a specific continental region. Moreover, to characterize a continental climate, it is essential to have information not only on surface temperatures, but also on precipitation and its seasonal polarity; such data cannot be directly derived from marine proxies.

In contrast to the marine realm, long quantitative climate records for the terrestrial realm are sparse. Palaeobotany-based records from the Paratethys (Ivanov *et al.* 2002; Mosbrugger *et al.* 2005; Syabryaj *et al.* 2007; Utescher *et al.* 2007) and the Cenozoic North Sea (Mosbrugger *et al.* 2005; Utescher *et al.* 2009) show that the long-term trends of climate evolution known from marine records are well reflected in continental curves. The North German records (Weisselster Basin, Lower Rhine Basin; cf. Utescher *et al.* 2009) are based on the analysis of macroflora, provide a high climatic resolution and when combined cover the time-span from the middle Eocene to the earliest Pleistocene. However, these records have a mean temporal resolution of only 1 Ma. Most Paratethys records mentioned above have a similar temporal resolution, except the microflora-based climate record of the Forecarpathian Basin by Ivanov *et al.* (2002) providing a higher resolution. Thus, short-term climate changes are only detected when the comparatively rare levels yielding macroflora are well positioned in a section. The Weisselster record shows a significant temperature drop at the Oligocene/Miocene transition that most probably corresponds to the Mi 1 glacial event (Mosbrugger *et al.* 2005). In general, however, a higher resolution is needed than macrofloras commonly provide to analyse short-term climate change and climate cycles in continental sections in order to study the coupling with high-frequency signals known from marine records.

Recently, a composite precipitation record for Central Europe has been presented based on herpetological proxies (Böhme *et al.* 2011). As quoted by the authors, the record has a resolution of down to 80 kyr and covers the time span from the Burdigalian to the Messinian. The record reveals pronounced alternations of mean annual precipitation varying between very wet phases with precipitation rates three times higher than at present and dry phases close to or below the limit for the existence of a closed forest cover. These phases, however, are not clearly correlated with marine isotope signals (Böhme *et al.* 2011). The record has been combined from mammal localities all over Central Europe and hence does not reflect precipitation evolution at any specific location.

A multi-proxy record was made available for two wells in the SE Netherlands by Donders *et al.* (2009). The marine succession the wells expose can be roughly correlated with the continental sections presented here. The study shows that decreases in sea-surface temperature broadly correlate with inferred third-order sea-level variations corresponding to oxygen-isotope glacial events Mi 3 through Mi 7. Curves for index variables derived from the palynomorph record show a coupling of marine and continental signals and changes from cool to warm conditions, or wet to dry, respectively, but the study provides no quantitative data.

Based on extensive studies of marine archives it is now widely accepted that not only the small-scale variability of marine records, e.g., of stable isotopes, Fe intensity or terrigenous components responds to orbital signals (e.g., Hilgen *et al.* 1995; Zachos *et al.* 2001; Holbourn *et al.* 2005). Also for longer-term changes on the scale of third-order sequences, orbital pacing is probable. Especially in the middle to late Miocene, glaciation events in most cases are shown to be associated with 400-kyr eccentricity minima and obliquity modulation minima (Westerhold *et al.* 2005). Thus, changes in high-latitude insolation have a direct impact on the formation of ice sheets in the Northern hemisphere.

In the present study, 5 palynomorph records from continental to shallow marine strata of the Lower Rhine Basin (NW Germany) covering the time span from the late Burdigalian to Zanclean are analysed with the Coexistence Approach, a quantitative technique to reconstruct palaeoclimate. The analysis aims at a more detailed view of small-scale climate variability in the continental area and its coupling with marine data. While marine proxies basically provide information on ocean water temperature, the palaeobotany-based reconstruction provides surface air temperatures including precipitation for the continental part and thus allows for the identification of climate type.

In our study the following questions are addressed:

- Are glacial events known from the marine realm coupled with the continental climate evolution? How sensitively do individual climate variables reflect these global changes in the study area and what amplitudes of change occur?
- Which cyclicities are reflected in the continental sections?
- How are the climate variables interrelated and how do they co-vary? Did these patterns change during the studied time span?
- How are the regional observations interpreted in terms of larger-scale changes of climate patterns?

Study Area

The Lower Rhine Basin (LRB) is a rift basin located in Northwest Germany which extends into the Cenozoic graben systems of The Netherlands and the North Sea. Deep penetrating tectonic faults subdivide the basin into different tectonic blocks, each having a different subsidence history (Figure 1). Sedimentation in the basin began with the Rupelian transgression. The Oligocene to Mid-Miocene sediment fill consists of up to 700 m coastal deposits interfingering with shallow marine sands towards the Northwest. The late early to middle Miocene continental strata in the Southeast comprise brown coal deposits of considerable economical importance. From the beginning of the late Miocene, fluviatile to lacustrine conditions prevailed in the basin (e.g., Zagwijn & Hager 1987; Hager & Prüfert 1988; Hager 1993; Schäfer *et al.* 2005; Figure 2).

Using both surface exposures and well logs, the structural geology and sedimentary facies of the LRB has been intensely studied. For an outline of more recent research in the basin see Schäfer *et al.* (2004, 2005). Most relevant for the present study is the availability of a sequence-stratigraphical concept provided for the Cenozoic fill of the LRB by the same authors. This concept has been compiled by considering the stratigraphical data available from various sources (e.g., nannoplankton, molluscs, forams, dinocysts, mammals, palaeomagnetics, radiometric dating; for a compilation see Schäfer *et al.* 2004). Based on these results, the entire succession was subdivided into a Rupelian to Serravallian transgressive systems tract, followed by a regressive systems tract with Tortonian to Pleistocene continental sediments (Schäfer *et al.* 2005; Figure 2). The SNQ 1 cored well was set up as stratigraphical standard to interpret local stratigraphy, based on hydrological units with code numbers according to Schneider & Thiele (1965), in the context of third order base-level stratigraphy (Schäfer *et al.* 2005). In many cases these base levels can be correlated with the interregional standard and with sequences of offshore successions in the adjacent North Sea Basin. New results obtained from dinocyst studies (see below) allow for a correlation of the Burdigalian to Serravallian part of our strata with the sequence concept set up by Rasmussen (2004) for the Eastern North Sea Basin.

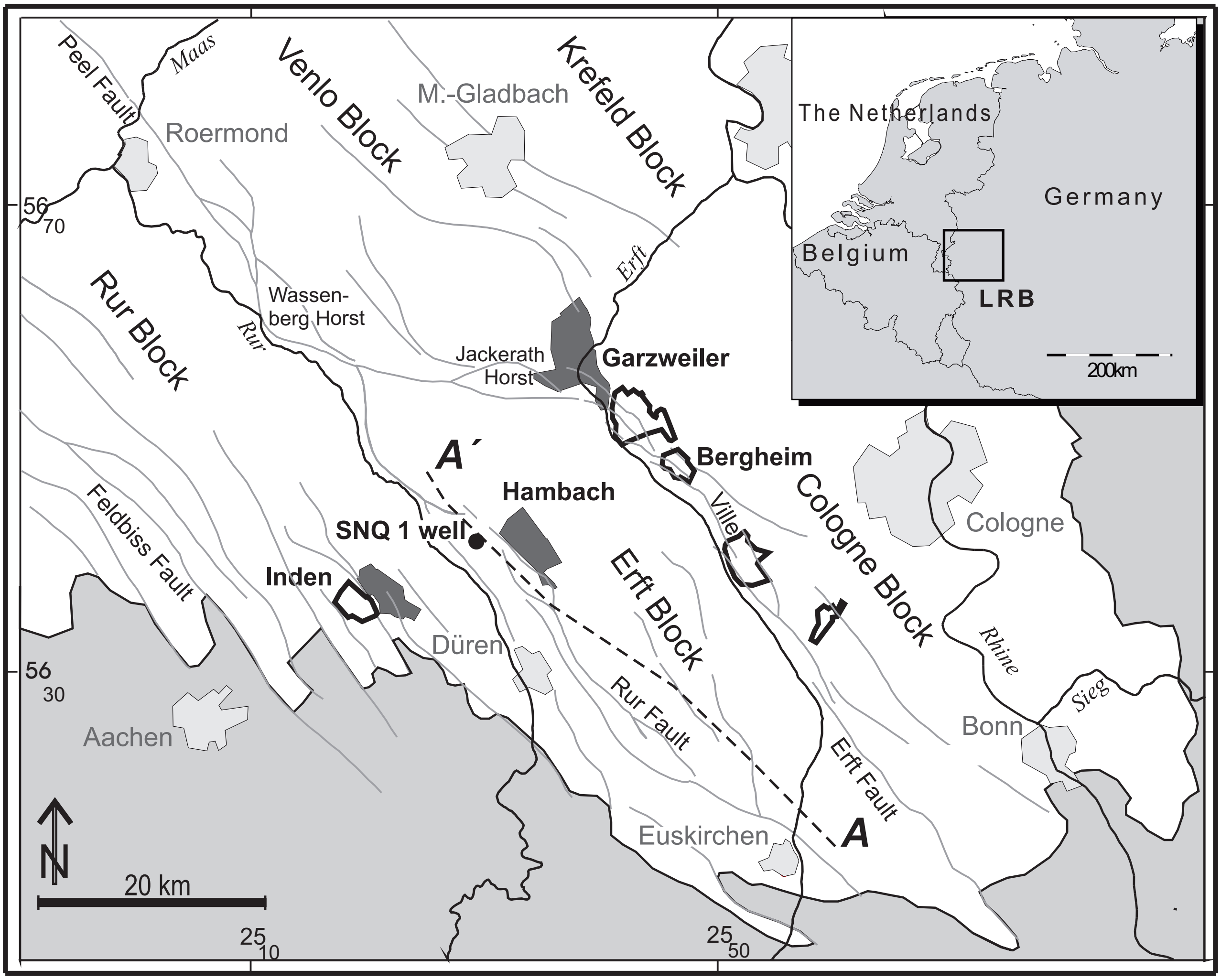

Figure 1. Study area and structural sketch map of the Lower Rhine Basin. Open cast mines indicated as solid are still active. A´–A– course of the cross-section of Figure 2.

Studied Sequences and Palynomorph Records

In the present study, palynological records from the stratigraphical standard, the SNQ 1 core, and from four correlated sections sampled at the Bergheim, Hambach, and Inden open cast mines are analysed. The sections in total cover the time span from the late Burdigalian to the Zanclean. The location of the sections is indicated in Figure 1, their stratigraphical position is shown in a facies scheme displaying the sedimentary evolution of the LRB during the Cenozoic (Figure 2). Various aspects of the Cenozoic palynological record of the LRB have been studied in detail (e.g., von der Brelie 1968; Zagwijn 1989; Van der Burgh & Zetter 1998; Kvaček *et al.* 2002). For the palynomorph record analysed here, pollen diagrams, palynostratigraphical data, and vegetation reconstructions are available in Ashraf & Mosbrugger (1995, 1996), Ashraf *et al.* (1997), Huhn *et al.* (1997 and Utescher *et al.* (1997). All the samples were processed according to Kaiser & Ashraf (1974) and Ashraf & Hartkopf-Fröder (1996). The number of counted grains was defined using rarefaction curves (cf. Ashraf & Mosbrugger 1995).

The palynological record of the SNQ 1 comprises 431 samples. However, the SNQ 1 sample series has various shortcomings when aiming at a detailed climate record. First of all, only the upper part of the well comprising Langhian and younger sediments

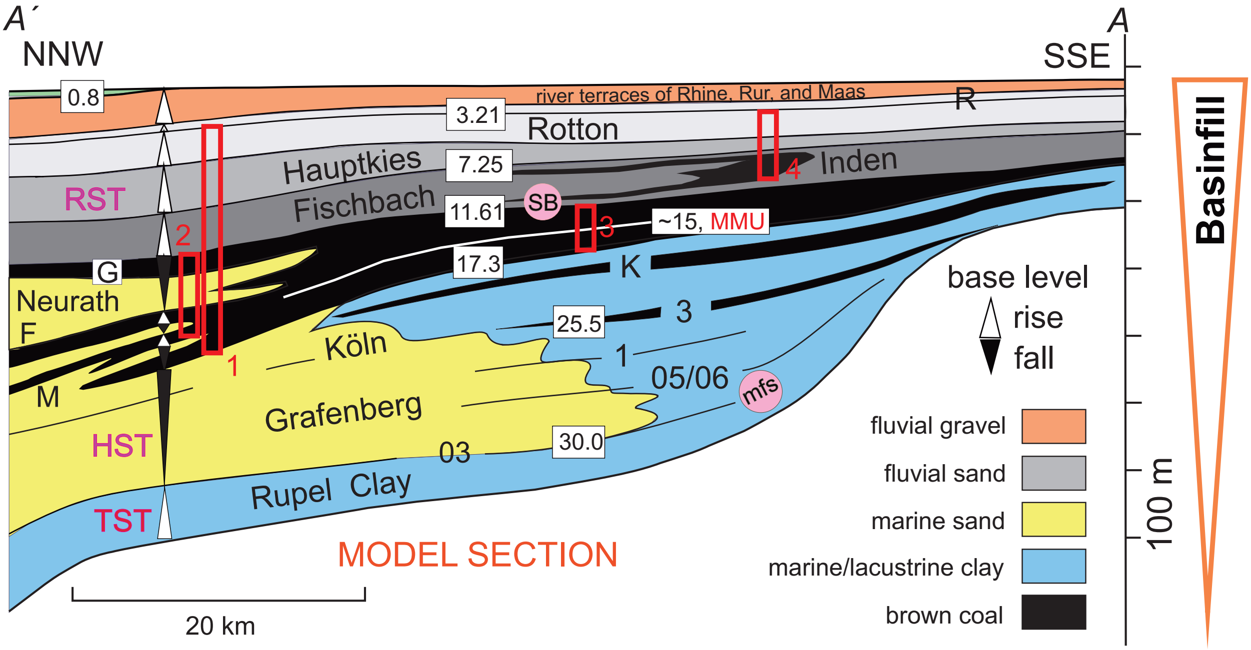

Figure 2. NNW–SSE-trending facies section (A´–A, indicated in Figure 1) of the Cenozoic fill of the Lower Rhine Basin with base-level concept and corresponding absolute ages indicated (from Schäfer *et al.* 2005, modified). TST– transgressive systems track; mfs– maximum flooding surface; HST– high stand systems track; SB– sequence boundary; MMU– Mid-Miocene Unconformity; RST– regressive systems track; black numbers refer to the local hydrological stratigraphy (Schneider & Thiele 1965); K– Kerpen Seam; M– Morken Seam; F– Frimmersdorf Seam; G– Garzweiler Seam; R– Reuver Clay. Red rectangles indicate the position of the studied sections. 1– SNQ 1 core; 2– Hambach section; 3– Bergheim section; 4– Inden Section.

has been cored, while for the Burdigalian to Mid-Miocene part only airlift samples are available. Also, series of samples are incomplete, especially in the brown coal part of the well, because here core legs had been taken for coal quality assessment and therefore could not be analysed for palynology. Secondly, the high subsidence rate in this part of the basin gave rise to the deposition of thick, coarse-grained horizons barren of palynomorphs. Therefore, the present study mainly relies on palynological data from correlated nearby profiles that do not cover the full stratigraphical range represented in the SNQ 1 core, but they do, at least in part, provide continuous records – in the case of thick brown coal sequences even undisturbed by facies change. In the following section we discuss the successions of the single stages.

Burdigalian to Serravallian

The Burdigalian to Serravallian part of the strata comprises coastal sands, namely the Morken Sand (hydrological horizon 5D), Frimmersdorf Sand (6B) and Neurath Sand (6D), each representing a sequence with base-level fall (Figures 2 & 3). Between the marine sands the Morken (6A), Frimmersdorf (6C) and Garzweiler (6E) brown coal seams are intercalated, as shown in the facies scheme (Figure 2). In each case, the peat bog evolved under a rising sea-level. The standard section (Figure 3) shows a clastic horizon within the Frimmersdorf Seam, the so-called 6Ca/b layer (Schäfer *et al.* 2004). From this horizon, a diverse vertebrate fauna was collected, dated as later MN5 (15.2–16 Ma; cf. Mörs *et al.* 2000; Mörs 2002). The Mid-Miocene ends with an erosional surface correlated with the Ser4/Tor1 sequence boundary where late Miocene fluviatile channels unconformably rest upon the brown coal (Schäfer *et al.* 2005). The Hambach section (Figure 3) can be correlated with the Mid-Miocene part of the SNQ 1 sequence and provided 237 palynomorph samples.

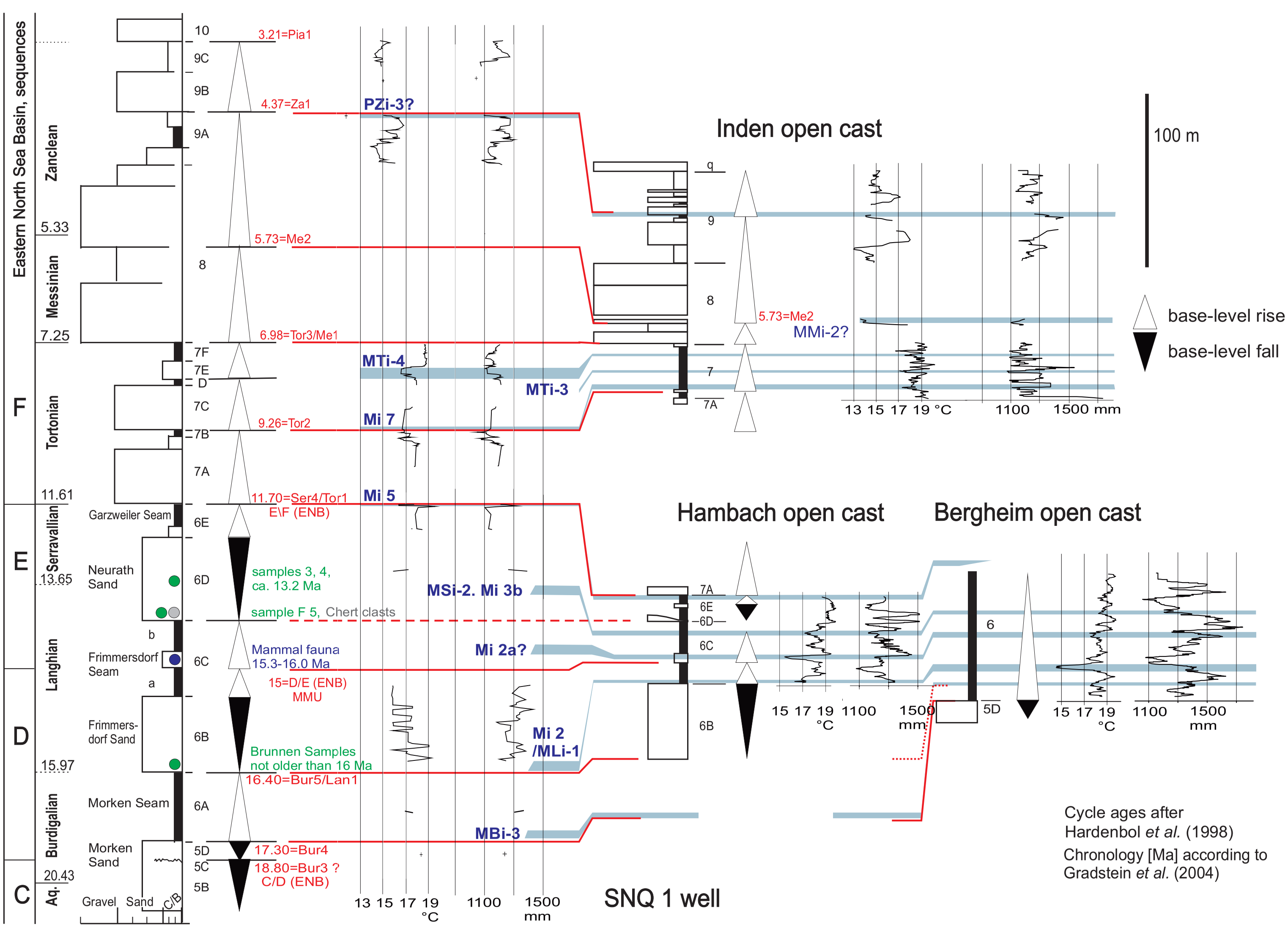

Figure 3. Grain size profiles of the studied sections with records for mean annual temperature (MAT, °C) and mean annual precipitation (MAP, mm). The curves are plotted for the means of CA intervals in each case using a gliding mean over ten samples. The numbering of the horizons refers to the hydrological stratigraphy (Schneider & Thiele 1965). Solid circles indicate the position of dinoflagellate samples analysed here. Lines connect base level cycles and third-order sequence boundaries according to Schäfer *et al.* (2005) following Hardenbol *et al.* (1998) adjusted to Gradstein *et al.* 2004), and sequence boundaries of the Eastern North Sea Basin (ENB) according to Rasmussen (2004) and the present study. MMU: Mid-Miocene Unconformity. Shaded levels refer to episodes of cooling partly connected to marine oxygen isotope events (cf. Figure 9).

In the former Bergheim open cast the latest Burdigalian to earlier Serravallian was represented by a single brown coal seam, up to 100 m thick, without any siliciclastic intercalations (Figure 3). From well log correlation it is known that the lower third of the Rhenish Main Seam in the Bergheim section approximately corresponds to the Morken Seam (6A horizon), the middle part of which is about equivalent with the marine sands of the 6B horizon and the Frimmersdorf Seam (6C), while the upper third of the Bergheim brown coal – rich in fossil woods – has equivalents in the marine sands of the 6D horizon and the Garzweiler Seam (6E) (Figure 3). The top of the brown coal again corresponds to the erosional event at the Ser4/Tor1 sequence boundary and the onset of fluviatile sedimentation in most parts of the basin, but was not reached in the measured section. 366 samples from this profile are presently analysed.

To enhance the stratigraphical concept, available so far for the early to middle Miocene part of the strata (Schäfer *et al.* 2004, 2005), new sample series have been collected from time-equivalent marine sands in the Garzweiler open cast to study organic-walled phytoplankton. These recent studies of dinoflagellate cysts and the new attempts of a sequence-stratigraphical correlation with the strata of the Eastern North Sea Basin (Rasmussen *et al.* 2010) require minor corrections in the Langhian of previous interpretation (Schäfer *et al.* 2005). Samples from the lowermost part of the Frimmersdorf Sand (6 B; Brunnen W 5309 borehole, 168.9–172.9 m) contain *Labyrinthodinium truncatum,* indicating an age not older than 16 Ma. According to Williams *et al.* (2004), the first occurrence of *L. truncatum* correlates with the Burdigalian–Langhian boundary, dated at 15.97 Ma by Gradstein *et al.* (2004). Following these considerations, the marine sands of the 5D horizon are correlated with the sea-level high stand following the Bur-3 third-order sequence boundary at around 18.8 Ma. This corresponds to the lower part of Sequence D in the sequence stratigraphy defined in the Eastern North Sea Basin (Rasmussen 2004). The overlying Morken Seam (6A) thus corresponds to the last Burdigalian third-order cycle succeeding the Bur-4 sea-level low stand. Hence, the base of the Frimmersdorf Sand (6B) represents a fourth-order flooding surface at around 16.0 Ma while the next sequence boundary has to be placed at the base of the incised fluviatile sediments (6C a/b horizon; see above) located in the middle of Frimmersdorf Seam (6C). According to new sequence-stratigraphical considerations and the time-frame provided by dinocyst zonation this level correlates with the D/E sequence boundary of the Eastern North Sea Basin. This boundary, widely distributed throughout the North Sea Basin, where it represents a ravinement surface represents the Mid-Miocene Unconformity (MMU) (Rasmussen *et al.* 2005, 2010; Köthe 2007; Köthe *et al.* 2008). Based on Sr isotopes the sequence boundary dates around 15.0 Ma.

According to Schäfer *et al.* (2004, 2005) the base of the marine Neurath Sand (6D) is interpreted as the Lan2/Ser1 third-order sequence boundary. At its base is a distinct layer containing angular chert clasts representing a transgressive surface. New dinoflagellate findings from this layer (at Garzweiler Mine) document the coexistence of *Labyrinthodinium truncatum* and *Cleistosphaeridium placacanthum*. Furthermore, the first occurrence of *Achomosphaera andalousiense* is found ca. 15 m above the base of the Neurath Sand (6D). These recordings strongly indicate that the trangressive phase should be referred to either the *Labyrinthodinium truncatum* Zone or the *Unipontidinium aquaductus* Zone of Dybkjær & Piasecki (2010) and that its age is Langhian to early Serravallian. To improve age control for the upper part of the Rhenish Main Seam, a dinoflagellate cyst study was carried out at the Garzweiler open cast mine on samples from the upper third of the Neurath Sand where the sands intercalate with the brown coals of the Garzweiler Seam, 6E (Figure 2). The coexistence of *Achomosphaera andalousiense* and *Cleistosphaeridium placacanthum* refers the studied interval to the *Achomosphaera andalousiense* Zone of Dybkjær & Piasecki (2010) and restricts the age to early to middle Serravallian (Powell and Brinkhuis 2004; Dybkjær & Piasecki 2010). These findings prove a Serravallian age for the upper part of the Rhenish Main Seam. It can be assumed that uppermost Serravallian sediments were partly eroded during the incision of the river system evolving during the Ser4/Tor1 sea-level low stand.

Tortonian and Messinian

The Upper Miocene in the LRB is characterized by fluvial, lacustrine and paludal conditions. The SNQ 1 record displays a sequence characteristic for the Erft Block in the central part of the basin (Figures 1 & 3), rapidly subsiding at that time with additional accommodation space provided by the compaction of the underlying Mid-Miocene brown coal. Three third-order sequences can be correlated with Tortonian cycles by sequence stratigraphy (Schäfer *et al.* 2005). Dinoflagellate cysts extracted from the upper third of the series support this stratigraphical concept (Strauss *et al.* 1993; NN11, ca. 5.6–8.5 Ma.). The strata consist of stacked fluviatile channels and floodplain deposits of a dominantly meandering river regime grading into lacustrine clays and peat bog facies, the so-called Upper Seam (Hager & Prüfert 1988). This succession is overlain by coarse-grained channel sediments of a braided river system (Hauptkies Series) marking a distinct northward progradation of the shoreline during the global sea-level low stand at the beginning of the Messinian (Schäfer *et al.* 2005). The late Miocene succession of the SNQ 1 well provided palynological data from about 100 samples. However, the record is rather fragmentary because the thick coarse-grained horizons provide no palynomorph materials while a continuous pollen record comprising 172 samples is available from a measured section in the Upper Seam, at Inden open cast (Figure 1; Ashraf *et al.* 1997). The lithological correlation with the standard section is based on the interpretation of well logs. The lowermost part of the Inden profile corresponds to clays and brown coal of the 7B horizon (Figure 3). The erosional basis of the fluvial channels of the 7C horizon on top corresponds to the Tor2 third-order sea-level low stand (9.26 Ma.), while the base of the overlying Hauptkies Formation (8 horizon) marks a major erosional phase correlated with the Tor3/Me1 sea-level low stand (6.98 Ma/7.25 Ma) indicating the beginning of the Messinian. The stratigraphical data outlined above allow for a rough estimate of the duration of peat formation. Brown coals of the Upper Seam about represent 2.6 Ma. When de-compacting the sequence a deposition rate of 2.39 cm / kyr is obtained (Table 1).

Zanclean

In the SNQ 1 core the Zanclean succession consists of ca. 60 m of sediments providing a palynomorph record of 137 samples. This so-called Rotton Series is subdivided into three hydrological horizons: 9A, 9B and 9C (Schneider & Thiele 1965). In the SNQ 1 well, the 9A horizon is a lacustrine fining-upwards sequence, connected to a pronounced global sea-level rise succeeding the Me2 low stand at ca. 5.5 Ma, while 9B and 9C are fluviatile deposits (Schäfer *et al.* 2005).

Age control in the section is based on the sequence stratigraphical concept for the LRB (Schäfer *et al.* 2004, 2005). According to this, the 9A horizon belongs to the upper part of the Me2 third order cycle, whereas the base of horizon 9B corresponds to the Za1 sea level low stand (at 4.37 Ma.). This interpretation is supported by dinocysts found in the upper part of the 9A horizon indicating NN12 (5.2–5.6 Ma; Strauss *et al.* 1993). According to Schäfer *et al.* (2005), the erosive base of the 10 horizon resting

Table 1. Cyclicities in the sections.

section	thickness of the sequence	number of cycles resolved/ estimated	time-span inferred from sequence-stratigraphical considerations	sedimentation rate assuming a decompaction factor of 3 (Hager *et al.* 1981)	cycle period
Hambach open cast, Frimmersdorf Seam, 0 m to 37 m	37 m	19/22	2.0 Ma	4.74. cm / kyr	105 kyr/ 90 kyr
Inden open cast, Upper Seam, 0 m to 32.7 m	32.7 m	19/23	2.6 Ma	3.77 cm / kyr	136 kyr/ 113 kyr

on top of the Rotton series can either be assigned to the first (Pia1= 3.21) or the second (Pia2= 2.76) Piacenzian third-order sea-level low stand.

A more complete palynomorph record was obtained from a ca. 50-m-thick sequence sampled at Inden open cast (117 samples). The profile does not show the threefold subdivision of the Rotton series which is frequently observed elsewhere in the LRB (Figure 3). The sampled part of the section starts with ca. 10 m of lacustrine clays overlain by sands and gravels of a braided river system, about time-equivalent with the 9B level in the SNQ 1 standard. Within this unit 3 fining upward sequences with intercalated silts, clays and brown coal are recorded, interpreted as oxbow lake deposits. These levels also yielded palynomorphs. In the upper part of the section, from depth level 111 m onwards, lacustrine conditions prevail, but single sandy channels and gravel layers reveal discontinuities in the record.

Methods

To reconstruct climate records from a total of about 1470 palynological samples the Coexistence Approach (CA) was used (Mosbrugger & Utescher 1997). The CA uses climatic requirements of all Nearest Living Relatives (NLRs) known for fossil macro or microflora to determine the climate range in which the palaeovegetation existed. To avoid potentially misleading results, samples with less than 50 non-saccate pollen grains were considered as not reliable and excluded from the analysis. A minimum threshold of eight identified NLR taxa together with climate data were set to include samples in the CA calculations, thus following the recommendation given in the methods description. Single occurrences of pollen grains were not taken into account. The selection of NLRs for the palynomorph taxa and corresponding climate data in general followed the latest version of the Palaeoflora data base (Utescher & Mosbrugger 2010). From various studies it is known that NLR taxa that have a relic status in present vegetation are problematic when being included in the CA calculations. Commonly such taxa exist in very restrictive climate conditions. Where such restrictive climate ranges are close to or within the climate range of most NLRs known for a flora they are not clearly identified as climatic outliers by the CA and may bias the results obtained. To avoid this effect, climate data for Taxodioideae were used for all pollen identified as *Sciadopityspollenites* and *Sequoiapollenites*.

In the present study, three temperature variables (mean annual temperature, MAT; cold month mean, CMT; warm month mean, WMT) and four precipitation variables (mean annual precipitation, MAP; monthly precipitation of the driest, wettest, and warmest month, MPdry, MPwet, MPwarm) were calculated for each microflora. To narrow down the variable ranges resulting from the CA all data are calibrated using the modern climatic space. The procedure follows the description given in Utescher *et al.* (2009). Modern climate range is defined here by six dimensions only, with MPwarm being not included. As modern climatology the New *et al.* (2002) data set was used. A software tool was developed to process large sample series. The software tool is a two step analysis tool. It first reads in a sample data set of fossil taxa and a table with all relevant temperature and precipitation data concerning these taxa. It constructs a table showing maximum and minimum temperature and precipitation for each sample. In a second step these maxima and minima are compared with a world climate data set and a geographical distribution is generated for each sample of the sample data set.

To visualize the results, series with higher-resolved records are shown for each section (Figures 4–7). For the summary of results presented in Figure 3, curves connecting means of CA intervals are shown, in each case using a gliding mean of ten samples. For the higher-resolved climate profiles means, partially with shaded area corresponding to the widths of CA ranges are shown using a gliding mean of 2. Climatic trends in the records are considered as significant when the mean values of a specific climate variable show a continuous decrease or increase over at least three data points.

Although the CA uses only the presence and absence of palynomorphs, a facies signal is certainly inherent to the climate records obtained. This is especially true for situations where the data field is comparatively unspecific, meaning that none of the NLRs identified for the fossil flora is close to its climatic limit under the fossil conditions. Assuming

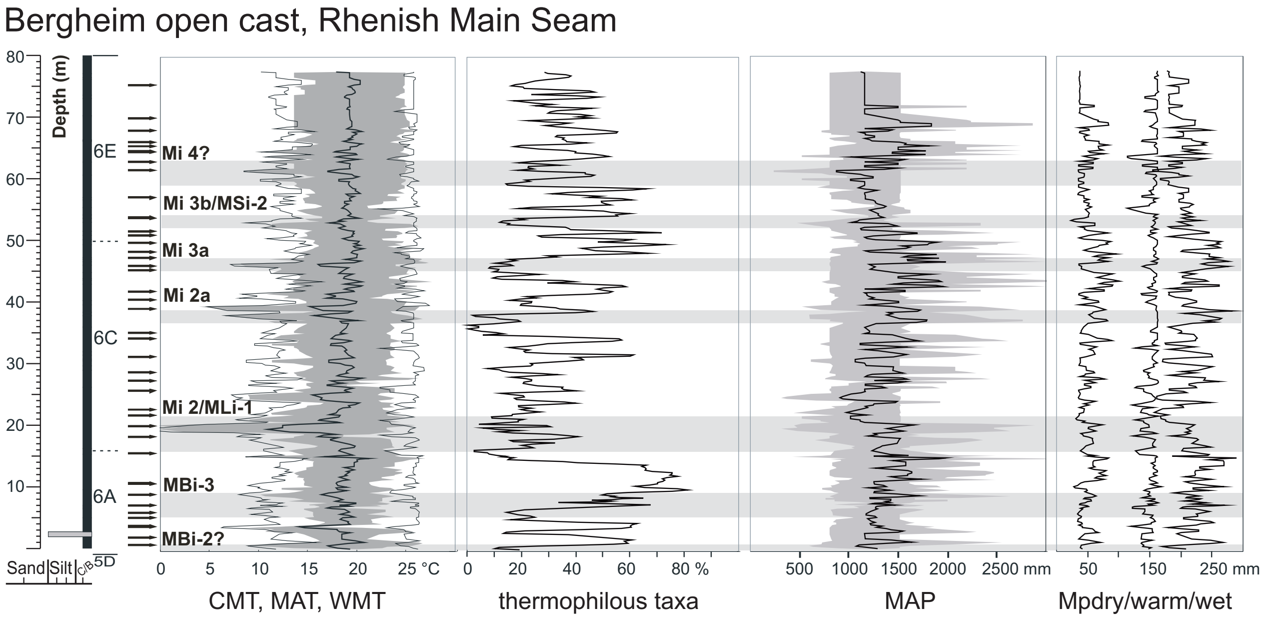

Figure 4. Grain size profile of the Rhenish Main Seam at the Bergheim open cast covering the time-span from the later Burdigalian to the Serravallian. 5D– Morken Sand; 6A– Morken Seam; 6C– Frimmersdorf Seam; 6E– Garzweiler Seam. Records for temperatures comprise three curves connecting CA interval means (CMT, MAT with shaded area according to the widths of CA ranges, and WMT) from left to right (°C), thermophilous components according Table 2 (%), mean annual precipitation (mm) with shaded area corresponding to CA interval widths, and monthly rainfall rates of the driest, the warmest and the wettest month (mm). Grey shaded levels refer to episodes of cooling connected to marine oxygen isotope events (cf. Figure 9). Arrows indicate small-scale cooling cycles. Grain size scale, C/B– clay, brown coal.

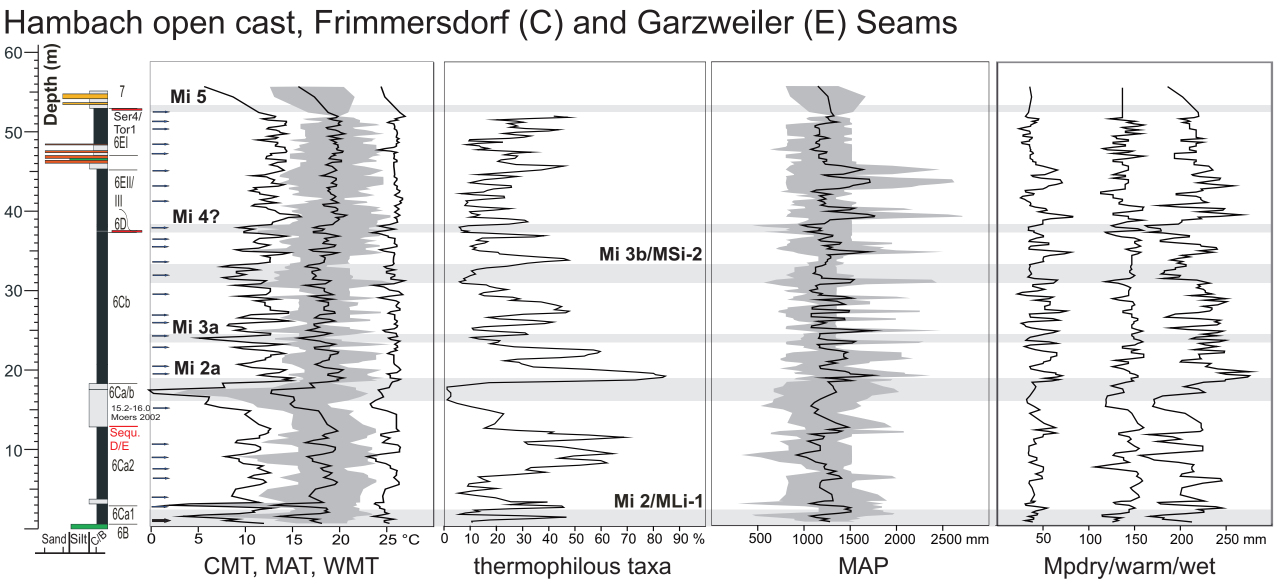

Figure 5. Grain size profile of the Langhian to earliest Tortonian succession at Hambach open cast. 6B– Frimmersdorf Sand; 6C– Frimmersdorf Seam; 6E– Garzweiler Seam; 7– Tortonian Fischbach Formation. For details on the records cf. Figure 4. Grey shaded horizons refer to episodes of cooling connected to marine oxygen isotope events (cf. Figures 3 & 9). Arrows indicate small-scale cooling cycles.

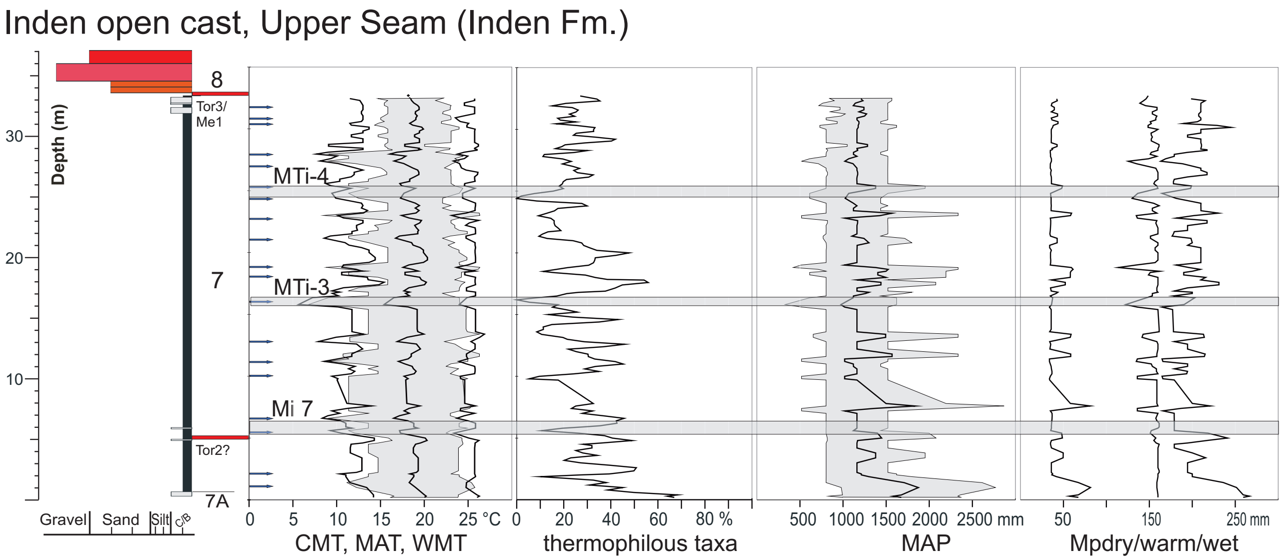

Figure 6. Grain size profile of the late Miocene sequence at the Inden open cast, including the Upper Seam (Tortonian; Horizon 7; Inden Formation) and the Hauptkies Series (Horizon 8; ~Messinian). For details on the records cf. Figure 4. Grey shaded horizons refer to episodes of cooling connected to marine oxygen isotope events (cf. Figures 3 & 9). Arrows indicate small-scale cooling cycles.

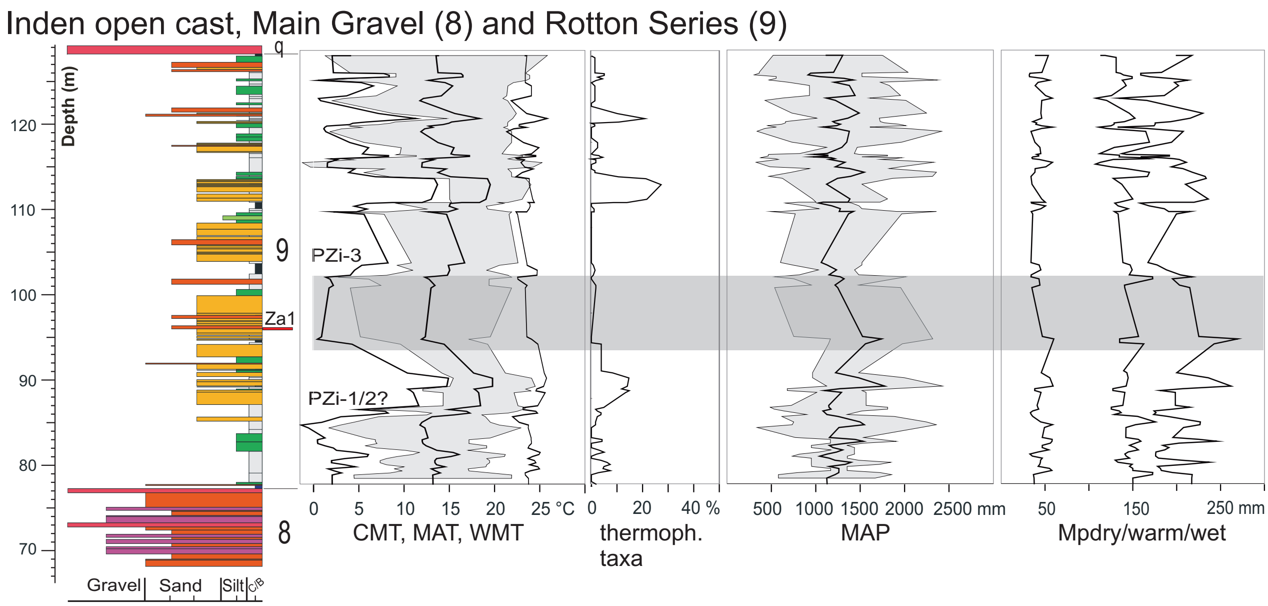

Figure 7. Grain size profile of the upper part of the Hauptkies Series (Horizon 8; ~Messinian) and the Zanclean Rotton Series (Horizon 9) of the Inden open cast. For details on the records cf. Figure 4. All records are smoothed using a gliding mean of 2. Grey shaded horizon refers to a cool episode connected to the marine PZi-3 oxygen isotope event (cf. Figures 3 & 9).

a change in edaphic conditions, e.g., from riparian to peat bog facies, a warm signal can be obtained, under the delimited taxonomical resolution palynomorphs provide. Typical Neogene mire vegetation includes many taxa that may exist under very warm climate conditions (e.g., Utescher *et al.* 2000), while in time-equivalent alluvial wetland vegetation deciduous taxa, restricted to more temperate climates, dominated (e.g., Kovar-Eder & Kvaček 2003).

To obtain a complementary signal, curves are presented showing percentages of a thermophilous group. The taxa allocated to this group are listed in Table 2; percentages are calculated from the non-saccate pollen sum (including spores). The thermophilous group also comprises pollen taxa with uncertain botanical affinity, but widely interpreted to indicate warm climate conditions. Being not closely related to any extant genera, these taxa provide no specific climate data sets for the CA (e.g., *Tricolporopollenites pseudocingulum, Quercoidites*

Table 2. Palynomorph taxa combined in the thermophilous group.

palynomorph taxon	**Nearest Living Relatives**
Arecipites convexus	Arecoideae
Arecipites monosulcoides	Arecoideae
Engelhardioipollenites punctatus	*Engelhardia*
Intratriporopollenites insculptus	Tilioideae, Brownlowioideae
Intratriporopollenites instructus	Tilioideae, Brownlowioideae
Platycaryapollenites miocaenicus	*Platycarya*
Porocolpopollenites orbis	*Symplocos*
Porocolpopollenites rarobaculatus	*Symplocos*
Porocolpopollenites rotundus	*Symplocos*
Quercoidites henrici	Fagaceae
Quercoidites microhenrici	Fagaceae
Reevesiapollis triangulus	*Reveesia*
Symplocoipollenites vestibulum ceciliensis	*Symplocos*
Symplocoipollenites vestibulum vestibulum	*Symplocos*
Tetracolporopollenites folliformis	Sapotaceae
Tetracolporopollenites manifestus contractus	Sapotaceae
Tetracolporopollenites manifestus ellipsoides	Sapotaceae
Tetracolporopollenites minimus	Sapotaceae
Tetracolporopollenites oblongus	Sapotaceae
Tetracolporopollenites obscurus	Sapotaceae
Tetracolporopollenites sapotoides	Sapotaceae
Tetracolporopollenites sculptatus	Sapotaceae
Tricolporopollenites cingulum oviformis	*Castanea, Castanopsis*
Tricolporopollenites cingulum pusillus	*Castanea, Castanopsis*
Tricolporopollenites edmundi s. Ashraf & Mosbrugger (1996)	Mastixiaceae
Tricolporopollenites marcodurensis	*Cissus, Parthenocissus*
Tricolporopollenites pseudocingulum	warmth loving angiosperm
Tricolporopollenites villensis	Cupuliferae (warmth loving)

microhenrici). Thus, the record of thermophilous taxa may unravel climate signals not resolved by the CA. However, it has to be remembered that the 'thermophilous records' of the present study primarily display a facies signal. To resolve palynomorph components whose frequency changes might best reflect temperature shifts, tests using multivariate ordination procedures were performed for taxa interpreted as thermophilous. These tests, however, turned out to be not very meaningful because it was shown that the warmth-loving floral components coexisted with changing plant associations during the time-span studied.

Results

Long-term Climate Trend

An overview of Burdigalian to Zanclean climate evolution and variability in the Cenozoic of NW Germany is best obtained using the summary curves obtained for MAT and MAP from the palynomorph record of the SNQ 1 standard and correlated sections (Figure 3). The MAT means vary between 13°C and 20°C, while the MAP means range from about 1000 to 1700 mm. Hence, warm and humid conditions persisted throughout the observed time span, even though the records show considerable small-scale variability of both temperature and precipitation parameters. This variability appears to be lowest during the early Serravallian (Hambach and Bergheim records) and in the Tortonian (Inden record), while Burdigalian to Langhian (SNQ 1, Bergheim and Hambach records) and Pliocene records (SNQ 1 and Inden records) reveal higher amplitudes of change. Although the climatic resolution of the CA is known to be comparatively low when based on microflora (see above), the records mirror the already known picture of long-term trends in climate evolution. The highest MAT (almost 20°C) occurred from the late Burdigalian to the early Serravallian, while during the Tortonian mean temperatures decreased to ca. 17°C. Near the top of the Tortonian a very warm phase is recorded. Pliocene data indicate cooler conditions with MAT around 15°C.

The MAP record of the SNQ 1 well shows a decreasing trend during the later Burdigalian, with rates falling from 1250 mm by a mean of ca. 100 mm. The Langhian to Serravallian parts of the records display a pointed variability with well expressed cycles from wetter to drier conditions, with MAP peaks attaining a mean of over 1500 mm. During the late Miocene, the MAP slightly decreased (Inden record) and then peaked again in the earlier Zanclean (SNQ 1 and Inden records); this MAP peak corresponds to the distinct warming during the sea-level rise pre-dating the Za1 sequence boundary. The later Zanclean is characterized by decreasing MAP (SNQ 1 and Inden records).

To elucidate short-term climate change, more highly resolved records (Figures 4–7) are described in the following.

Short-term Climate Change

Burdigalian to Serravallian: The Rhenish Main Seam at Bergheim and Hambach Open Cast – The Burdigalian to Serravallian temperature records obtained for both sections resolve no distinct, longer-term temperature change, but all variables display an increasing stability towards the later Langhian and Serravallian part of the sections (Figures 3–5). In addition to the small-scale variability, several longer-lasting cool phases are recorded. These phases, indicated by bars in the figures, can be correlated in part with glacial events known from marine isotope stratigraphy and are discussed in Discussion section on 'Climate Events and Their Correlation with Sequence Stratigraphy and Marine Oxygen Isotope Record'. The most distinct event in the Bergheim record, around the depth level 20 m, corresponds to a ca. 5-m-thick brown coal bed. Here cooling is also well expressed in declining summer temperatures. Proportions of thermophilous components show a sharp drop of percentages. Another punctuated cool episode is present at the depth level around 38 m in the Bergheim section (middle part of Frimmersdorf Seam, Langhian); here, a very strong signal is evident for the CMT. This second event has to be correlated with the most prominent event recorded in the Hambach section, at the depth level from 16 to 18 m. Again, temperature decrease corresponds to a sharp drop in proportions of thermophilous taxa. Towards the top of the sections (upper part of Frimmersdorf Seam, late Langhian to earlier Serravallian), temperatures became altogether more stable. As is obvious from the precipitation data, cool episodes frequently start with a sharp decrease in MAP (e.g., depth levels at 16 m and 38 m in the Bergheim record), then in most cases followed by a trend to wetter conditions.

In the Burdigalian to Serravallian precipitation records, the Bergheim section displays four distinct cycles with alternating wetter and drier phases; in the Hambach records, the three upper cycles are present. These cycles culminate at depths of ca. 15, 28, 46, and 64 m at Bergheim, and 6, 19, and 48 m at Hambach, respectively. While MAT, MPdry, and MPwet change almost in parallel, MPwarm stays more or less constant. This invokes the striking effect that the MPwet and the MPwarm curves repeatedly converge, especially during some of the major cooling phases (e.g., at depth levels 22 m and 60 m in the Bergheim record), meaning that climate shifted to conditions with highest precipitation rates in the warm season. In the available stratigraphic data, each of the longer-term precipitation cycles represents about 400 kyr (Table 1, Figure 9).

Short-term climate variability in the records is best reflected by CMT and MAT. In the Bergheim record, 39 cooling cycles are identified in total, whereas there are 28 cooling cycles recorded in the Hambach section (cf. Figures 4 & 5, arrows). Cycle thickness varies between 0.80 m and 2 m at Bergheim, and between 1 m and 2.5 m in the Hambach record. The small-scale cycles partly show a regular pattern; at some levels cycles may be present, but they are not clearly resolved in the palaeoclimate reconstruction. This is probably due to unrecognized discontinuities.

Precipitation records also display some short-term variability. As is obvious from the curves obtained, short-term cool phases coincide with higher seasonality of temperature and altogether drier conditions (MAP; MPwet). In the precipitation records, it is shown that cooling is often connected to drying (Figure 3). Hence, very wet intervals are frequently connected to high temperatures (e.g., depth levels 19 m; 40 m of the Hambach record). In some cases, however, shifts in precipitation rates cannot be related to any temperature change (depth levels 6 m, 13 m, 44 m of the Hambach section).

Based on the number of around 20 small-scale cycles recorded from the Frimmersdorf Seam at Hambach open cast and the time frame assumed (see above; Table 1), these climate variations most probably represent 100-kyr cycles paced by eccentricity of the earth's orbit.

Using microfloras that commonly do not provide a high climatic resolution, a quantification of short-term climate changes is mostly impossible. A temperature change of at least 0.1°C is documented for MAT, at depth levels 15.45 m, 24.2 m, and 26 m of the Hambach record. A MAP increase of at least 50 mm is evident at depth level 39.50 m; MPwet and MPdry significantly changed by at least 20 mm and 10 mm, respectively (depth levels 51–53 m, 42 m, 34 m, 30 m, 26.2 m, Hambach record).

Tortonian: The Upper Seam at Inden Open Cast – The Tortonian record is based on 127 palynological samples from the Upper Seam, ca. 34 m thick (Figure 6). It also shows small-scale climate variability, but amplitudes of change appear to be altogether smaller than the Langhian records (see above). The Inden record displays four longer-term cycles evident from shifts in temperature, the proportion of thermophilous elements, and in MPwet. Cool phases are recorded at depth levels 6 m, 16 m, and 26 m. In each case cooling affects all temperature variables studied. The cooling events at depth levels 16 m and 26 m begin with a pointed drop and subsequent increase of precipitation rates. The curves for MPwarm and MPwet both indicate a climate type with highest rainfall rates during summer. While in the middle Miocene there is occasional evidence for such conditions (see above), wet summers obviously were more common in the Tortonian.

Tortonian small-scale climate variability is shown by cycles between ca. 0.8 m and 2 m thick. 19 cycles are evident from the climate curves over the whole Inden section; 23 when taking into account shifting proportions of thermophilous components. Amongst temperature variables CMT again has the highest variability but climate conditions were generally more stable than in the Langhian/Serravallian (see above). As in the middle Miocene, cooling commonly is connected to drying.

Assuming about 2.6 Ma as the time frame for the formation of the Upper Seam (see above), the

Tortonian cycles each represent about 100 kyr and are also related to eccentricity (Table 1).

Quantification of short-term climate change is successful at depth level 28.5 m where a drop of at least 3°C is evident. In all other cases temperature and precipitation changes are not quantifiable.

Zanclean: The 9 Horizon at the Inden Open Cast and in the SNQ1 Core – Frequent facies changes and irregularly spaced samples complicate the interpretation of both Zanclean records from the LRB. As stated above, temperatures were altogether cooler than Miocene conditions, and precipitation rates were slightly lower. The variability of the temperature parameters studied is higher than during the Tortonian; for the first time, the WMT shows distinct oscillations. Although the record exhibits no distinct long-term climate trend (see above), the CMT shows a slight decreasing trend, while the mean annual range of temperature (MART) increased towards top of the Rotton Formation.

The Zanclean temperature records reveal several distinct cool phases. A significant cooling is shown at depth level 82 m of the Inden record, correlated with coarsening of the sediments (Figure 7). In the SNQ 1 core, a potentially time-equivalent cool phase is present at depth level –160 m. In both cases, this cooling was connected to increasing precipitation. The cool episode was followed by distinct warming, expressed in all temperature variables studied. In the middle part of the 9 horizon of the Inden section our data show part of a warming cycle. The upper part of the Inden record displays regular cycles at 2–3 m intervals. Warmer intervals again roughly correspond to a coarsening of the siliciclastic component, but a closer look reveals that the onset of the warming already occurred within the clays and therefore should not be connected to the presence of reworked components. The SNQ 1 record provided no samples that can be regarded as time-equivalent to the middle part of Zanclean succession of the Inden open cast. Samples from the silts in the uppermost part of the Rotton Series in the SNQ 1 well reveal 2 small-scale climate cycles, although correlation with the Inden record is not possible.

Unlike during the Miocene, cool intervals tended to be wetter or to start with wet conditions while in most cases warming was connected to drying (e.g., at depth levels 86 m; 95 m, 110 m, 116 m of the Inden section; Figure 7). Small-scale temperature cycles of about 1 m thickness are evident in the brown coal seam of the SNQ1 record (depth level 140–150 m; Figure 3). In the other parts of the sequence such cycles are not displayed, obviously due to frequent facies changes and heterogeneous sedimentation rates. The early Pliocene records of thermophilous taxa are in perfect accordance with the temperature records of both sections. The strong decline in the proportion of these components when compared to the late Miocene is evident (Figure 7).

Discussion

Reconstructed Curves Compared to Other Continental Climate Records

Due to the relatively low climatic resolution of the CA obtained from microfloras (e.g., Utescher *et al.* 2000), the quantification of climate change is less precise than data obtained from macrofloras, even when calibrating data using modern climate space (Utescher *et al.* 2009; Figures 8 & 9). Macrofloras, in turn, commonly are too scarce in the sedimentary record to allow for the assessment of smaller-scale change.

From the latest Burdigalian to the Serravallian, a MAT of 18.3°C results from the microfloras when averaging means obtained from all samples (Figure 9), a value close to the macroflora-based data (17.8–19.6°C: cf. Utescher *et al.* 2009). The reconstructed mean MAP of 1375 mm (Figure 8) is slightly higher than the calculation based on macroflora remains (flora Neurath Sand, code f, Utescher *et al.* 2009: 1247 mm), but coincides with the data calculated for the Garzweiler flora (code g; 1231–1356 mm). Comparatively dry conditions with MAP ranging from 800 to 900 mm reconstructed for a Langhian macroflora originating from the Frimmersdorf Seam (presence of *Ocotea*, cf. Utescher *et al.* 2000) are also present in coeval parts of the Bergheim section. In the drier episode recorded at the depth level 20 m minima of CA ranges drop to values around 500 mm (Figures 4 & 8). The warming towards the Mid-Miocene Climatic Optimum (Zachos *et al.* 2001) is also expressed in the microflora-based reconstruction (Figure 9). However, the onset of the longer-term Late Miocene Cooling – evident in the macro-record

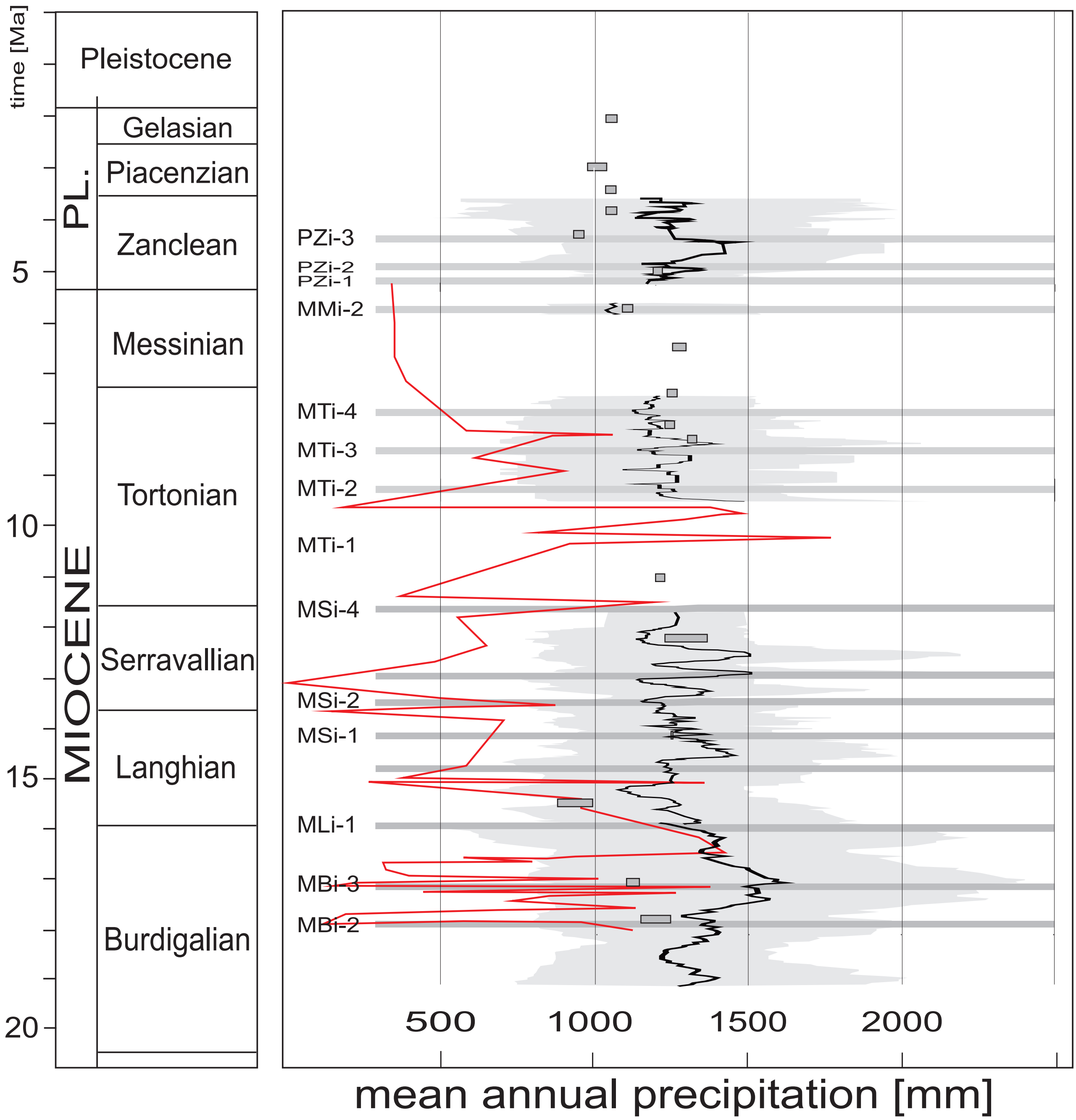

Figure 8. Mean annual precipitation records for the time-span from the Burdigalian to Zanclean. Composite record (single parts explained in Figure 9) obtained from microflora (this study). The grey shaded areas correspond to the widths of coexistence intervals, the curves connect interval means and are smoothed using a gliding mean of 10. Grey boxes represent MAP ranges obtained from macroflora of the LRB (from Utescher *et al.* 2009). Solid curve on the left. Precipitation record reconstructed from herpetological assemblages for Central Europe (from Böhme *et al.* 2011). Grey shaded levels indicate episodes of cooling connected to marine oxygen isotope events (cf. Figure 9).

from climate data reconstructed from a fruit and seed flora from the Serravallian Garzweiler Seam (6E) – is not clearly resolved in temperature records from the microflora (cf. Hambach, Bergheim; Figures 4, 5 & 9). In the Northern Atlantic distinct cooling began with the Mi 4 isotope event at ca. 13 Ma (cf. Miller

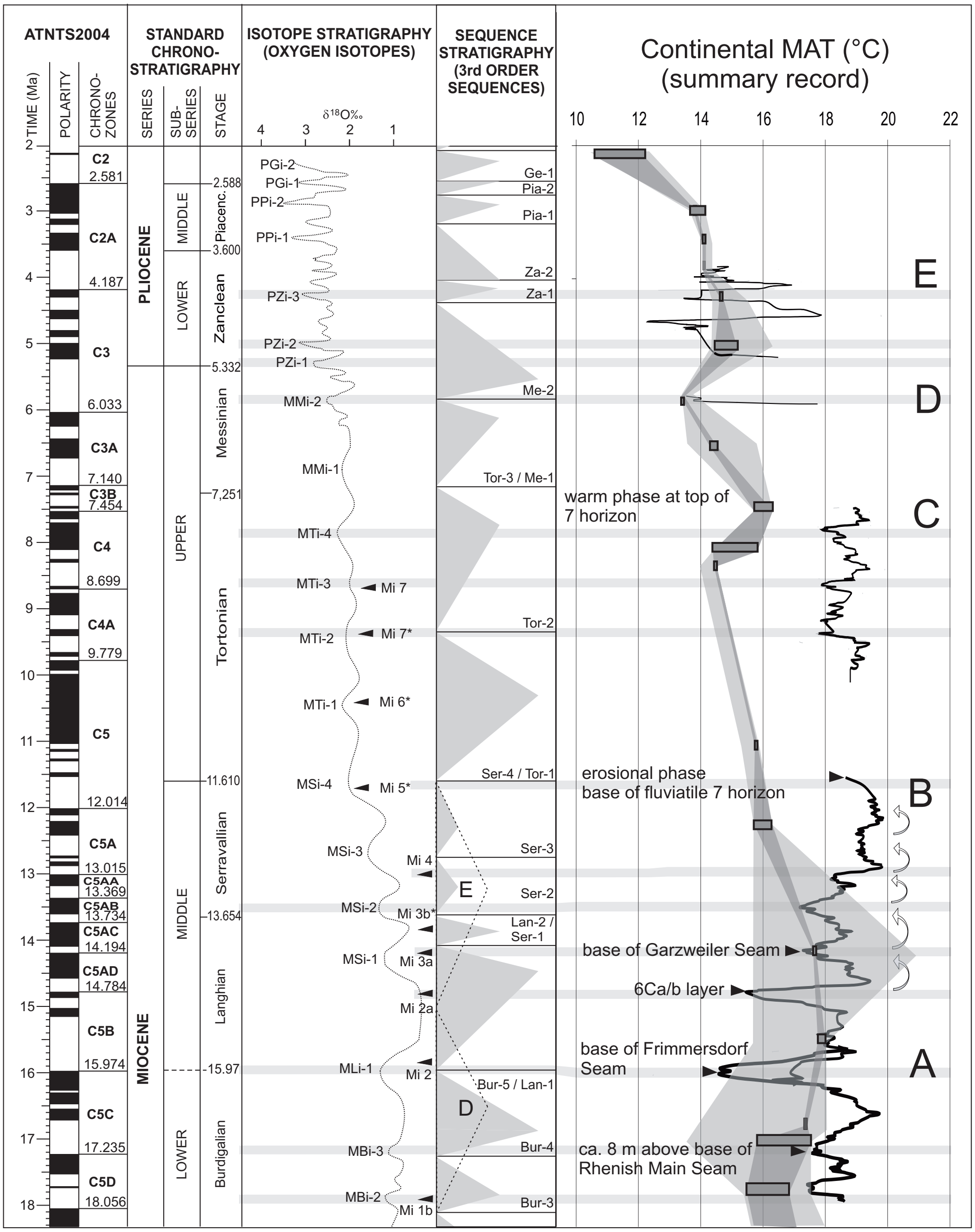

Figure 9. Neogene chronostratigraphy modified from Harzhauser & Piller (2007). Oxygen isotope stratigraphy after Abreu & Haddad (1998), Mi events according to Miller *et al.* (1998); *) orbitally tuned Mi events according to Shackleton *et al.* (1999), Turco *et al.* (2001), Abels *et al.* (2005), and Westerhold *et al.* (2005); sequence stratigraphy after Hardenbol *et al.* (1998), and after Rasmussen (2004) for the Eastern North Sea Basin; all zones recalibrated according to Gradstein *et al.* (2004) and Lourens *et al.* (2004), and continental mean annual temperature records for NW Germany (summary). Solid black line: data from this study. The curves are plotted for means of CA intervals using a gliding mean of ten samples. A– Bergheim record; B– Hambach record; C, D, E– records from the Inden open cast. Arrows indicate 400 kyr cycles in the later Langhian and Serravallian. Grey bars and shaded area: MAT record from Utescher *et al.* (2009) based on macroflora from the LRB.

et al. 1991). In the Bergheim record (Figure 4) CMM and contents of thermophilous components decline in the uppermost Serravallian from depth level 65 m on. About 12 m above the MSi-2 event (13.5 Ma), the Hambach record (Figure 5) displays a comparable small-scale cyclicity, but means of CA intervals show an increasing trend. This observed discrepancy reveals certain weaknesses when quantifying longer-term climate trends with microflora and underlines the importance of complementary CA analyses based on the macrofloral record (cf. also see also next chapter for discussion).

The Tortonian record based on microflora, sampled from the lignites of the Upper Seam, shows an offset of MAT means towards warmer conditions (around 18.7°C averaged over all CA interval means) when compared to the results obtained from macroflora where 15.7°C to 16.3°C are obtained (Hambach 7F; cf. Utescher *et al.* 2009; Figure 9). However, CA ranges show that the results do not contradict each other. The reason for this offset is most probably because various taxa with warm climatic requirements are still present in the late Miocene flora; temperate elements in turn are assigned to NLRs at the generic level while fruits and seeds and leaf flora partly allow for comparison at species level (e.g., Van der Burgh 1988; Belz & Mosbrugger 1994). Since many typical temperate genera also have representatives in warm temperate climates CA ranges are thus not delimited towards their warm ends.

With regard to precipitation, there is better agreement between MAP data calculated from macroflora and MAP means obtained from the microflora. With a MAP of 1226 mm averaged over all CA interval means, precipitation rates were slightly lower than in the Mid-Miocene. Again, these data are very close to the macroflora-based reconstruction (1231–1327 mm; flora codes h – j; Utescher *et al.* 2009; Figure 8). The marked CMT increase documented in the macrofloral record at the top of the Tortonian is also reflected in the microflora-based reconstruction (Figure 9).

The discrepancies between climate data derived from micro- and macrofloras, as observed for temperature, certainly could also be related to differing taphonomical conditions such as transport from afar and/or provenance of the materials from higher altitudes (e.g., Kvaček *et al.* 2006). In the late Miocene palaeogeographical settings of our study area this factor might be not so critical. At that time, a low, peneplained Palaeozoic block bordered the basin and the river system had a restricted catchment area (e.g., Schäfer *et al.* 2005).

The microflora-based Zanclean climate record is more variable than the record obtained from macroflora (Figures 8 & 9). However, both records show a marked warming and increase of precipitation rates during the first Zanclean cycle. Data published for the early Zanclean macroflora (1212 mm – 1214 mm, code l; Utescher *et al.* 2009) are similar to the present results. As with the macroflora record, the present curves display subsequent cooling and drying, in addition to shorter-term cyclicity not resolved by the macroflora. While precipitation decrease in the later Zaclean is expressed in both the macro and microflora record (Figure 8), microfloral means show an offset to wetter conditions by ca. 200 mm. As with the offset of temperature in the Tortonian, this can be explained by unspecific NLR allocation when employing microflora (see above). However, a MAP around 900 mm reconstructed from macroflora is not in conflict with the microfloral data when considering the full CA ranges (Figures 7 & 8).

Furthermore, reconstructed precipitation curves can be compared to a continental MAP record based on the ecophysiological structure of herpetological assemblages (Böhme *et al.* 2011; Figure 8). The record represents a summary reconstructed from Central and Eastern European sites and covers the time span from the late Burdigalian to the Messinian. With a mean resolution of 200 ka quoted by the authors the record is more detailed than the record based on macroflora (Utescher *et al.* 2009) and provides an independent time control based on mammal zonation. When this curve is compared with our summary record on Figure 8 a considerable offset of both data fields is obvious. Very high amplitudes of change, as indicated by the vertebrate record, showing dry pulses with annual rainfall rates falling below 500 mm, as in the Burdigalian, later Langhian to earlier Serravallian and also the middle part of the Tortonian, were not present in NW Germany according to our palaeobotany-based reconstruction. As obvious from the minima of CA ranges (cf.

summary record, Figure 8) MAP clearly stayed above 600 mm throughout the time-span studied. In addition, no evidence in our palynomorph record points to the existence of steppe conditions prevailing outside the basin. Since the Lower Rhine Basin was part of the so-called Central European wet zone (van Dam 2006) and probably had a climate with a relatively strong oceanic imprint, these findings are not surprising and do not necessarily negate the existence of very dry intervals elsewhere in Central Europe, e.g., in the Central Paratethys.

Climate Events and Their Correlation with Sequence Stratigraphy and Marine Oxygen Isotope Record

All records studied, especially those from the brown coal sections where signals are not perturbed by facies change, show distinct climate cooling events occurring at more or less regular intervals. Considering the available stratigraphical frame and time control in the sections, these events are within the scale of third-order sequences and stable-isotope events described from marine records. This coupling is shown in Figure 9 where our continental MAT curves are plotted against the chronological standard showing sequence stratigraphy after Hardenbol *et al.* (1998) recalibrated according to Gradstein *et al.* (2004) and Lourens *et al.* (2004), and the oxygen isotope stratigraphy after Abreu & Haddad (1998), with Mi events according to Miller *et al.* (1991, 1998), Sugarman *et al.* (1997), Shackleton *et al.* (1999), Turco *et al.* (2001), Abels *et al.* (2005), and Westerhold *et al.* (2005). For the summary record MAT curves for the Bergheim (A) and Hambach (B) sections are combined for the Burdigalian to Serravallian part: for the late Miocene and early Pliocene curves of the Inden record are shown (C, D, E, cf. Figure 9). All curves are adjusted to the time scale according to the sequence-stratigraphical constraints outline in section on 'Studied Sequece and Palynomorph Record', Studied Sequences and Palynomorph Records (cf. Figure 3) and smoothed using a gliding mean of 10 samples.

When accepting the correlation of the Morken Sand (5D) with the sea level high stand of Sequence D in the sequence stratigraphical concept for the Eastern North Sea Basin (cf. chapter 3.1), the MBi-3 event is reflected in the Bergheim record, closely above the base of Horizon 6, the Rhenish Main Seam (Figure 3). Increasing temperatures and percentages of thermophilous components in the brown coals equivalent to the Morken Seam correspond to the base-level rise predating the Bur5/Lan1 sequence boundary at ca. 16 Ma. The Mi 2 event is evident in the SNQ 1 record, at the base of the Frimmersdorf Seam. It is also recorded in the Hambach section, at the depth level between 16 m to 19 m, showing a sharp drop in temperature combined with decreasing proportions of thermophilous taxa while rainfall increased. In the Bergheim section, the Mi 2 event is recorded between 17.5 m and 21 m. Continental signals indicating the Mi 2 event have already been described by Donders *et al.* (2009) based on a multi-proxy study on two wells from the Venlo Block in The Netherlands. The wells, Groote Heide and Heumensord, allow for the study of shallow-marine time-equivalents of the LRB strata. The subsequent cooling event observed within the Langhian (Frimmersdorf Seam), at a level correlated with the D/E sequence boundary of the Eastern North Sea Basin (see above), possibly correlates with a sharp declining peak reported from the oxygen isotope record of Site 747 at 14.8 Ma described by Sugarman *et al.* (1997) as the Mi 2a event (Figure 9). The high amplitude of climate change inferred in the Hambach record can partly be explained by an additional imprint of facies change reinforcing the signal (Figure 5). The Bergheim record shows a much weaker pulse. Again, the rising base level as proposed by Schäfer *et al.* (2005) for the 6Cb Frimmersdorf Seam coincides with rising temperatures. The later Langhian to Serravallian part of the MAT record (B on Figure 9) displays at least 3 additional cooling events that correspond with marine signals (MSi-1/Mi 3a, MSi-2, Mi 4).

In the shallow marine facies exposed in the Dutch wells, Donders *et al.* (2009) identified two heavy isotope events in the late Langhian to Serravallian part of their records (Mi 3/Mi 3b; Mi 4). The Mi 4 event is present in the Hambach record, at depth level 38 m (Figure 5) while the SNQ 1 well provides no data in this part of the profile. Mi 3b is orbitally tuned and has an absolute age of 13.82 Ma (Westerhold *et al.* 2005).

Temperatures and precipitation decrease observed in all records right below the base of the late Miocene

7 horizon (Inden Formation) cannot be clearly related to the global sea-level low stand at the Ser-4/Tor-1 sequence boundary corresponding to the Mi 5 heavy isotope event at 11.7 Ma (age astronomically calibrated; Westerhold *et al.* 2005). Our records are discontinuous at that level, crossing an erosional surface, in parts deeply incised, in part obvious from compacted peat surfaces bored by marine molluscs (e.g., Schäfer *et al.* 2005). In the more continuous marine records of the SE Netherlands not only isotope data but also continental proxies reflect the Mi 5 signal (Donders *et al.* 2009).

Our Tortonian sequence, the approximately 30 m thick Upper Seam (Figure 6), also provides a climate record undisturbed by facies change. When following the above stratigraphical considerations (see section on 'Studied Sequence and Palyrological Record: Tortonian and Messinian'), the MTi-2 (~Mi7) to MTi-4 isotope events (Miller *et al.* 1991; Abreu & Anderson 1998; Westerhold *et al.* 2005) are mirrored in the continental climate record. However, the interpretation is complicated by the fact that the correlation of the MTi events with orbitally calibrated Mi events is still a matter of debate (Westerhold *et al.* 2005). The records by Donders *et al.* (2009) show a very distinct SST signal for the Mi 7 event when alternatively assuming a possible 9.4 Ma age, as proposed by Westerhold *et al.* (2005). Continental proxies from the Dutch wells, in contrast, show no signal at that level. The cold phase indicated by Donders *et al.* (2009) for the time span between 7.5 Ma and 8.6 Ma most probably corresponds to the profile part between 17–29 m in the Inden section (Figure 6). While the authors show only one single, longer persisting cooling our data show two distinct events that would support the Abreu & Anderson (1998) version (Figure 9). Although not really quantifiable, the Donders *et al.* (2009) records allow for tracing the very warm short-term phase above the MTi-4 event from the southern Lower Rhine area to the Northwest. This warm phase has long been known and is connected to widespread peat formation in the LRB (Schophofen Seam, horizon 7F) (cf. Utescher *et al.* 2000). In the continental climate late Miocene glaciation events show an imprint on all temperature variables studied. While during the MTi-2 event precipitation data show almost no signal, both younger events caused significant drying (cf. MAP signal on Figure 6).

In the Zanclean records frequent facies changes with numerous erosional surfaces present, combined with the scarcity of independent stratigraphical dating, complicates the identification of isotope events. Cooling, setting in at the base of the 9A horizon in the SNQ 1 core (Figure 3) and at 81.5 m in the Rotton section of the Inden open cast (Figure 7), culminating at ca. 150 m in the SNQ and at 84.5 m at Inden, respectively, is most probably correlated with one of the two distinct isotope events in the early Zanclean (PZi-1; PZi-2). In both sections rainfall rates show increasing trends during cooling. There is some evidence for a cool phase near the Za1 third-order sequence boundary in both Zanclean records (Figures 3 & 7) but both records are intermittent at that level.

Climate Cycles and Variability of Climate

The cyclic recurrence of cool periods in the records is obviously related in a number of cases to glacioeustatic events (Mi events according to Miller *et al.* 1991) as outlined above. The sensitivity of this continental region to reflect signals known from marine records has been known before (Utescher *et al.* 2000; Donders *et al.* 2009). In the middle to late Miocene glacioeustatic Mi events are clearly related to orbital forcing which allows for their precise age calibration. As shown by Westerhold *et al.* (2005) the oxygen isotope events can be correlated with minima in the 400 kyr band of the eccentricity cycle in combination with minima in the 174 kyr obliquity modulation. Cycles with periods of around 400 kyr are well expressed in the later Langhian to Serravallian part of the MAT record of the Hambach open cast (cf. arrows on Figure, 9). Thus late Langhian to early Serravallian continental records of the LRB most probably show temperature changes responding to eccentricity-modulated variations in precession. A strong impact of the 400 kyr cycle on Miocene ocean temperature was reported by Zachos *et al.* (2001) and also by Westerhold *et al.* (2005) and characterises time-spans with unipolar glaciation.

The numerous small-scale cycles observed in the climate records of the Burdigalian to Serravallian brown coals do not show a particularly regular pattern because subsidence and sedimentation rate were obviously not constant. Considering the total number of cycles and the given time frame, the data strongly point to a 100 kyr cyclicity (eccentricity) of short-term climate change (Table 1). It is known from various, marine records that orbital forcing is often well expressed in Mid-Miocene successions, for example from the Paratethys and Tethys where it is derived from various proxies (e.g., Hilgen *et al.* 1995; Brandano *et al.* 2005; Hohenegger *et al.* 2009; Lirer *et al.* 2009).

In the Tortonian brown coal section of the Inden open cast, about 19 small-scale climate cycles were observed (Figure 6). Assuming a time-span of 2.5 Ma represented (see section on 'Studied Sequences and Palynomorph Records: Tortonian and Messinian'; Figure 9), these data again point to the 100 kyr band of eccentricity. The fact that 100 kyr cyclicity is expressed in the Tortonian part of our record fits well with observations by Holbourn *et al.* (2007) that, from the glaciation at the end of the Monterey Event on, climate change was mainly triggered by eccentricity. Climate proxy records from sedimentary successions from the northwestern and southeastern Pacific (ODP Sites 1146 and 1237) show a pointed 100 ka variability from 13.9 Ma onwards. The 100 kyr cyclicity is also described from the Monte dei Corvi reference section of the Tortonian (Hüsing *et al.* 2009) where it is supposed that, as in the Pleistocene, the 100-kyr cycles are the driving force for the fluctuations in ice-sheet expansion on the Northern Hemisphere, first evident from the appearance of Ice-rafted Debris (IRD) at 12.6 Ma (Westerhold *et al.* 2005).

The evolution of climate variability can be quantified interpreting the standard deviation of the single variables in terms of amplitudes of cyclic changes. A comparison of variability obtained for different variables is not meaningful in this context because it is strongly dependent on the co-domain of the parameter. Therefore changes in variability through time are discussed. The evolution of climate variability is shown in the Figures 10 and 11 for the Langhian/Serravallian, Tortonian, and Zanclean time spans. With temperature parameters it is shown that variability did obviously not increase from the Mid-Miocene to the late Miocene as would have been expected as a consequence of the onset of NH glaciation (e.g., Westerhold *et al.* 2005). According to the present data late Miocene conditions even tended to be more stable than the Mid-Miocene. However, marine isotope records, e.g. the d^{18}O record of ODP site 1237 (Holbourn *et al.* 2007), indicate higher variability and amplitudes during the Langhian (~16 to 14.6 Ma) in which variability is characterized by high-amplitudes of 100 kyr variability and by prominent 400 kyr oscillations in δ^{13}C that follow the Earth's long eccentricity band. Late Miocene oxygen isotope records show smaller amplitudes of change, such as the composite global oxygen isotope record between 11 and 9 Ma (cf. Westerhold *et al.* 2005; Figure 6). This is also true for the amplitude of eustatic sea level changes (e.g., Miller *et al.* 2005). In particular, the variability of MPdry declined when compared to that during the Langhian.

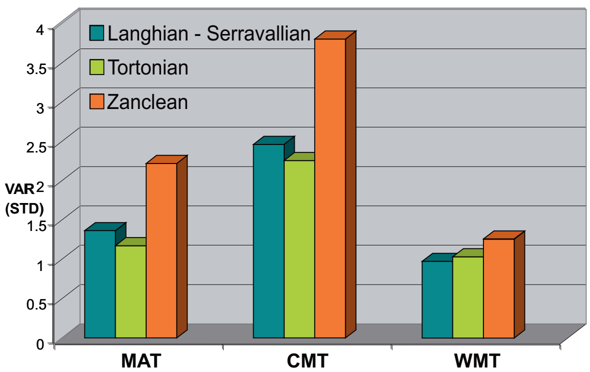

Figure 10. Evolution of MAT, CMT and WMT variability in NW Germany from the Langhian to the Zanclean. Calculations of the standard deviation are based on the Bergheim and Inden sample series.

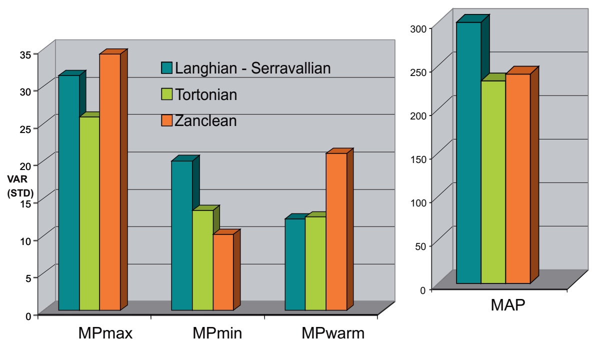

Figure 11. Evolution of precipitation variabilities in NW Germany from the Langhian to the Zanclean. Calculations of the standard deviation are based on the Bergheim and Inden sample series.

The Pliocene climate show overall higher variability of temperature parameters, which is most marked in CMT. Possibly the continental climates of the Pliocene LRB reacted very sensitively to shifts in the Northern Atlantic circulation, although the early Pliocene provided globally warm condition, possibly even a permanent El Nino (Fedorov *et al.* 2006), prior to the Quaternary-style oscillations between glaciations and interglacials since ca. 2.3 Ma ago (Sarnthein *et al.* 2009).

The correlation panel (Figure 12) illustrates the covariance of the single climate parameters presently studied. A comparison of climate data obtained from the Langhian/Serravallian of the Bergheim record with Tortonian and Zanclean data (both from the Inden record) shows that Langhian/Serravallian, and Tortonian patterns of the correlation matrices are very similar, while the early Pliocene matrix is strikingly different. In the Miocene, warming was clearly connected to a wetter climate, especially the increase of summer precipitation (MPwarm) and rainfall rates of the wettest season (MPwet) as shown by the high positive correlation. This could be related to a comparatively strong orbital pacing of climate changes causing alternations of periods with equable / seasonal rainfall.

In the early Pliocene, in contrast, warming obviously had no significant impact on rainfall rates, or was even connected to drier conditions, especially during the dry season (MPdry), thus causing a pointed seasonal aspect of precipitation distribution throughout the year. In particular, the relation between WMT increase and MPwarm decrease is noteworthy. Similar observations are made from tree-ring analysis in the early Pliocene of Ellesmere Island indicating alternating intervals of cool/wet to warm/dry conditions, but changes occur there on a suborbital scale (Csank *et al.* 2007). Other processes are not yet clear. A distinct dry summer season was not established in Western Europe and Southern Italy before 2.6 Ma. Quaternary-type Mediterranean climatic cycles started at approximately 2.3 Ma (Bertini 2001). However, a trend to drier summers in Western Europe (e.g., Catalonia), is evident from early Pliocene palaeovegetation data (Kovar-Eder *et al.* 2006), although all these regions are at lower latitude than our study area.

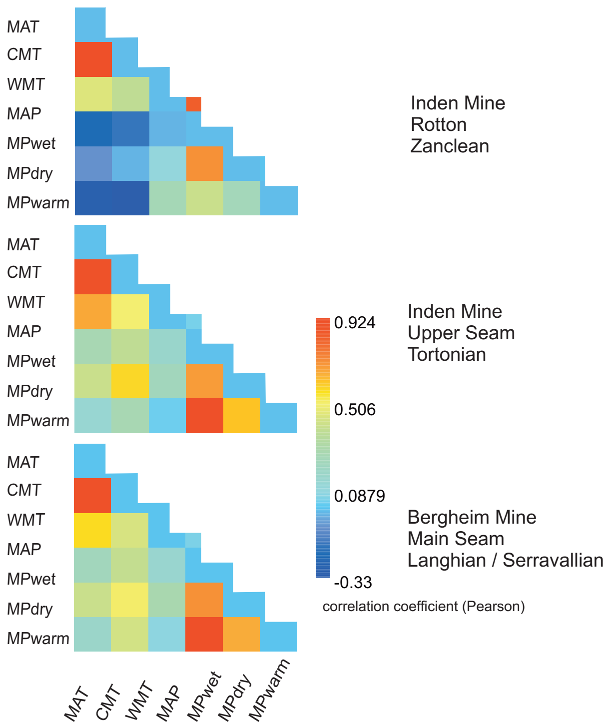

Figure 12. Colour-coded correlation panel showing Pearson correlation coefficients obtained from correlation analysis for the climate variables MAT, CMT, WMT, MAP, MPwet, MPdry, and MPwarm. The coefficients are based on 275 Langhian to Serravallian (Bergheim section), 144 Tortonian, and 96 Zanclean climate data sets (both from the Inden section). Dark blue–negative correlation; brighter blue to green– not correlated; brighter green to red– positive correlation.

Summary and Conclusions

As shown in the present study, palaeoclimate analysis of microfloras by the Coexistence Approach is well suited to obtain detailed quantitative records for various variables allowing for a detailed analysis of continental climate evolution. Our results show a quite obvious coupling of continental temperatures with marine SSTs. Many of the Neogene glaciation events known from marine isotope signals are mirrored in the continental curves. While marine records do not allow direct assessment of climate variables, palaeobotany-based data are suitable to reconstruct Neogene climate types because the main key variables are available. It is shown that in this continental position in the mid-latitudes of the NH cold month mean temperatures react most sensitively to global climate change over the observed time-span. Precipitation, especially rainfall rates of the wettest month, is highly variable; in the later early Pliocene variability of rainfall rates of the warmest month increases.

In spite of the calibration technique applied, the exact quantification of climate change remains problematic in most cases. However, this problem cannot be overcome because the comparatively low taxonomical resolution in identifying Nearest Living Relatives for the fossil taxa does not allow for distinctly identifying taxa delimiting the warm ends of the climate data field obtained from a sample.

In Neogene climate records from NW Germany, by small-scale climate changes are, as shown by this study, primarily triggered by orbital forcing and – as known from marine records – change their relevance through the time-span studied. Small-scale climate variability observed in our Burdigalian to Tortonian records can be referred to a 100 kyr eccentricity while in the later part of the Langhian and in the Serravallian, 400 kyr cycles are as well expressed.

The analysis of inter-relations of climate variables provides insight into shifts of the climate system over the time-span studied. During the period from the Burdigalian to the Tortonian the functioning of the climate system did not change significantly, but our data indicate a substantial change for the early Pliocene. The Miocene climate of NW Germany was characterized by warm and wet / cool and dry cycles, while in the early Pliocene warm periods tended to have dry summers.

Acknowledgements

We thank our colleagues for many fruitful discussions. We are indebted to A. Schäfer (Bonn) and E.S. Rasmussen (Copenhagen) for their kind advice concerning sequence stratigraphy and sedimentology. We express our thanks to R.W.E. Power for supporting our field work and providing materials. The financial support of the German Science Foundation (DFG, Mo 412/240-1) the Biodiversity and Climate Research Center (BIK-F) of the Hessian Initiative for Scientific and Economic Excellence (LOEWE) are gratefully acknowledged. Finally, warm thanks go to our three anonymous reviewers for their very constructive comments and helpful corrections. This study is a contribution to the NECLIME (Neogene climate evolution of Eurasia) network.

References

Abels, H.A., Hilgen, F.J., Krijgsman,W., Kruk, R.W., Raffi, I., Turco, E. & Zachariasse,W.J. 2005. Long-period orbital control on middle Miocene global cooling: integrated stratigraphy and astronomical tuning of the Blue Clay Formation on Malta. *Paleoceanography* **20**, PA4012.

Abreu, V.S. & Anderson, J.B. 1998. Glacial eustasy during the Cenozoic; sequence stratigraphic implications. *American Association of Petroleum Geologists Bulletin* **82**, 1385–1400.

Abreu, V.S. & Haddad, G.H. 1998. Glacioeustatic fluctuations: The mechanism linking stable isotope events and sequence stratigraphy from the early Oligocene to middle Miocene. *SEPM Special Publication* **60**, 245–259.

Ashraf, A.R. & Hartkopf-Fröder, C. 1996. Die Siebverfahren bei der Aufbereitung palynologischer Proben. *Neues Jahrbuch für Geologie und Paläontologie, Abhandlungen* **200**, 221–235.

Ashraf, A.R. & Mosbrugger, V. 1995. Palynologie und Palynostratigraphie in Niederrhein. Bucht Teil 1. Sporen. *Palaeontographica B* **235**, 61–173.

Ashraf, A.R. & Mosbrugger, V. 1996. Palynologie und Palynostratigraphie in der Niederrheinischen Bucht. Teil 2 Pollen. *Palaeontographica B* **241**, 1–98.

Ashraf, A.R., Mosbrugger, V. & Utescher, T. 1997. Palynological studies in the Neogene of the open pit mines Inden and Bergheim. Lower Rhine Embayment (Germany). *Courier Forschungsinstitut Senckenberg* **201**, 29–46.

Belz, G. & Mosbrugger, V. 1994. Systematisch-paläoökologische und paläoklimatische Analyse von Blattfloren im Mio-/Pliozän der Niederrheinischen Bucht (NW-Deutschland). *Palaeontographica B* **233**, 19–156.

Bertini, A. 2001. Pliocene climatic cycles and altitudinal forest development from 2.7 Ma in the Northern Apennines (Italy): evidence from the pollen record of the Stirone section (5.1 to 2.2 Ma). *Geobios* **34**, 253–265.

Böhme, M., Winklhofer, M. & Ilg, A. 2011. Miocene precipitation in Europe: temporal trends and spatial gradients. *Palaeogeography, Palaeoclimatology, Palaeoecology* **304**, 212–218. doi:10.1016/j.palaeo.2010.09.028.

Brandano, M., Corda, L. & Mariotti, G. 2005. Orbital forcing recorded in subtidal cycles from a Lower Miocene siliciclastic–carbonate ramp system, (Central Italy). *Terra Nova* **17**, 434–441.

Csank, A.Z., Patterson, W.P., Eglington, B., Basinger, J.F. & Rybczynski, N. 2007. Climate variability in a Pliocene boreal forest: evidence from tree-rings of sub-fossil wood. *American Geophysical Union Fall Meeting 2007, Abstract* PP51E-03.

Donders, T.H., Weijers, J.W.H., Munsterman, D.K., Kloosterboer van Hoeve, M.L., Buckles, L.K., Pancost, R.D., Schouten, S., Sinninghe, J.S., Damsté, J.S.S. & Brinkhuis, B. 2009. Strong climate coupling of terrestrial and marine environments in the Miocene of northwest Europe. *Earth and Planetary Science Letters* **281**, 215–225.

Dybkjær, K. & Piasecki, S. 2010. Neogene dinocyst Zonation for the Eastern North Sea Basin, Denmark. *Review of Palaeobotany and Palynology* **161**, 1–29.

Fedorov, A.V., Dekens, P.S., McCarthy, M., Ravelo, A.C., deMenocal, P.B., Barreiro, M., Pacanowski, C. & Philander, G. 2006. The Pliocene Paradox (Mechanisms for a Permanent El Niño). *Science* **312**, 1485–1489.

Gradstein, J.G., Ogg, J.G. & Smith, A.G. (eds) 2004. *A Geologic Time Scale*. Cambridge University Press.

Hager, H. 1981. Das Tertiär des Rheinischen Braunkohlenreviers – Ergebnisse und Probleme. *Fortschritte der Geologie im Rheinland und Westfalen* **29**, 529–564.

Hager, H. 1993. The origin of the Tertiary lignite deposits in the Lower Rhine Region, Germany. *International Journal of Coal Geology* **23**, 251–262.

Hager, H., Kothen, H. & Spann, R. 1981. Zur Setzung der rheinischen Braunkohle und ihrer klastischen Begleitschichten. *Fortschritte der Geologie im Rheinland und Westfalen* **29**, 319–352.

Hager, H. & Prüfert, J. 1988. Tertiär. *In*: Hilden, H.D. (ed), *Geologie am Niederrhein*. Geologisches Landesamt Nordrhein-Westfalen, , Krefeld, 32–40.

Hardenbol, J., De Graciansky, C., Jacquin, T. & Vail, P.R. (eds) 1998. *Mesozoic and Cenozoic Sequence Stratigraphy of European Basins*. SEPM Special Publications **60**, 1–485.

Harzhauser, M. & Piller, W.E. 2007. Palaeogeography, Palaeobiogeography and events in the Central Paratethys during the Miocene. *Palaeogeography, Palaeoclimatology, Palaeoecology* **253**, 8–31.

Hilgen, F.J., Krijgsman, W., Langereis, C.G., Lourens, L.J., Santarelli A. & Zachariasse, W.J. 1995. Extending the astronomical (polarity) time scale into the Miocene. *Earth and Planetary Science Letters* **136**, 495–510.

Hohenegger, J., Rögl, F., Coric, S, Pervesler, P., Lirer, F., Roetzel, R., Scholger, R. & Stingl, K. 2009. The Styrian Basin: a key to the middle Miocene (Badenian/Langhian) Central Paratethys transgressions. *Austrian Journal of Earth Sciences* **102**, 102–132.

Holbourn, A., Kuhnt, W., Schulz, M. & Erlenkeuser, M. 2005. Impacts of orbital forcing and atmospheric carbon dioxide on Miocene ice-sheet expansion. *Letters to Nature* **438**, 483–487.

Holbourn, A., Kuhnt, W., Schulz, M., Flores, J.A. & Andersen, N. 2007. Orbitally-paced climate evolution during the middle Miocene 'Monterey' carbon-isotope excursion. *Earth and Planetary Science Letters* **261**, 534–550.

Huhn, B., Utescher T., Ashraf, A.R. & Mosbrugger, V. 1997. The peat-forming vegetation in the Middle Miocene Lower Rhine embayment, an analysis based on palynological data. *Mededelingen Nederlands Institut voor Toegepaste Geowetenschappen TNO* **58**, 211–218.

Hüsing, S.K., Kuiper, K.F., Link, W., Hilgen, F.J. & Krijgsman, W. 2009. The upper Tortonian–lower Messinian at Monte dei Corvi (Northern Apennines, Italy): completing a Mediterranean reference section for the Tortonian Stage. *Earth and Planetary Science Letters* **282**, 140–57.

Ivanov, D., Ashraf, A.R., Mosbrugger, V. & Palamarev, E. 2002. Palynological evidence for Miocene climate change in the Forecarpathian Basin (Central Paratethys, NW Bulgaria). *Palaeogeography, Palaeoclimatology, Palaeoecology* **178**, 19–37.

Kaiser, H. & Ashraf, A.R. 1974. Gewinnung und Präparation fossiler Sporen und Pollen sowie anderer Palynomorphae unter besonderer Betonung der Siebmethode. *Geologisches Jahrbuch* **25**, 85–114.

Köthe, A. 2007. Cenozoic biostratigraphy from the German North Sea sector (G-11-1 borehole, dinoflagellate cysts, calcareous nannoplankton). *Zeitschrift der Deutschen Gesellschaft für Geowissenschaften* **158**, 287–327.

Köthe, A., Gaedicke, C. & Lutz, R. 2008. Erratum: The age of the Mid-Miocene Unconformity (MMU) in the G-11-1borehole, German North Sea sector. *Zeitschrift der Deutschen Gesellschaft für Geowissenschaften* **159**, 687–689.

Kovar-Eder, J. & Kvaček, Z. 2003. Towards vegetation mapping based on the fossil plant record. Acta Universitatis Carolinae. *Geologica* **46**, 7–13.

Kovar-Eder, J., Kvaček, Z., Martinetto, E. & Roiron, P. 2006. Late Miocene to early Pliocene vegetation of southern Europe (7–4 Ma) as reflected in the megafossil plant record. *Palaeogeography, Palaeoclimatology, Palaeoecology* **238**, 321–339.

Kvaček, Z.M., Kovác, Kovar-Eder, J., Doláková, N., Jechorek, H., Parashiv, V., Kovačová, M. & Sliva, L. 2006. Miocene evolution of landscape and vegetation in the Central Paratethys. *Geologica Carpathica* **57**, 295–310.

Kvaček, Z., Manchester, S.R., Zetter, R. & Pingen, M. 2002. Fruits and seeds of *Craigia bronnii* (Malvaceae-Tilioideae) and associated flower buds from the late Miocene Inden Formation, Lower Rhine Basin, Germany. *Review of Palaeobotanyand Palynology* **119**, 311–324.

Lirer, F., Harzhauser, M., Pelosi, N., Piller, W.E., Schmid, H.P. & Sprovieri, M. 2009. Astronomically forced teleconnection between Paratethyan and Mediterranean sediments during the middle and late Miocene. *Palaeogeography, Palaeoclimatology, Palaeoecology* **275**, 1–13.

LOURENS, L., HILGEN, F., SHACKLETON, N.J., LASKAR, J. & WILSON, J. 2004. Orbital tuning calibrations and conversions for the Neogene Period. *In*: GRADSTEIN, F.M., OGG, J.G. & SMITH, A.G. (eds), *A Geologic Time Scale 2004*. Cambridge University Press, 469–471.

MILLER, K.G., KOMINZ, M.A., BROWNING, J.V., WRIGHT, J.D., MOUNTAIN, G.S., KATZ, M.E., SUGARMAN, P.J., CRAMER, B.S., CHRISTIE-BLICK, N. & PEKAR, S.F. 2005. The Phanerozoic record of global sea-level change. *Science* **310**, 1293–1298.

MILLER, K.G., MOUNTAIN, G.S., BROWNING, J.V., KOMINZ, M., SUGARMAN, P.J., CHRISTIE-BLICK, N. & KATZ, M.E. 1998. Cenozoic global sea level, sequences, and the New Jersey transect: results from coastal plain and continental slope drilling. *Review of Geophysics* **36**, 569–601.

MILLER, K.G., WRIGHT, J.D. & FAIRBANKS, R.G. 1991. Unlocking the icehouse: Oligocene–Miocene oxygen isotope, eustacy, and margin erosion. *Journal of Geophysical Research* **96**, 6829–6848.

MÖRS, T. 2002. Biostratigraphy and palaeoecology of continental Tertiary vertebrate faunas in the Lower Rhine Embayment (NW Germany). *In*: SCHÄFER, A. & SIEHL, A. (eds), *Rift Tectonics and Syngenetic Sedimentation – the Cenozoic Lower Rhine Graben and Related Structures*. Netherlands Journal of Geosciences, Geologie en Mijnbouw **81**, 177–183.

MÖRS, T., VON DER HOCHT, F. & WUTZLER, B. 2000. Die erste Wirbeltierfauna aus der miozänen Braunkohle der Niederrheinischen Bucht (Ville-Schichten Tagebau Hambach). *Paläontologische Zeitschrift* **74**, 145–170.

MOSBRUGGER, V. & UTESCHER, T. 1997. The coexistence approach – a method for quantitative reconstructions of Tertiary terrestrial palaeoclimate data using plant fossils. *Palaeogeography, Palaeoclimatology, Palaeoecology* **134**, 61–86.

MOSBRUGGER, V., UTESCHER, T. & DILCHER, D.L. 2005. Cenozoic continental climatic evolution of Central Europe. *Proceedings of the National Academy of Sciences* **102**, 14964–14969.

NEW, M., LISTER, D., HULME, M. & MAKIN, I. 2002. A high-resolution data set of surface climate over global land areas. *Climate Research* **21**, 1–25.

POWELL, A.J. & BRINKHUIS, H. 2004. Paleogene dinoflagellate cyst zonation and datums and radiolarian zonation, with their estimated correlation to magnetostratigraphy and calcareous nannoplankton zones. *In*: GRADSTEIN, F.M., OGG, J.G. & SMITH, A.G. (eds), *A Geologic Time Scale 2004*. Cambridge University Press, Cambridge, 395–396.

RASMUSSEN, E.S. 2004. Stratigraphy and depositional evolution of the uppermost Oligocene–Miocene succession in western Denmark. *Bulletin of the Geological Society of Denmark* **51**, 89–109.

RASMUSSEN, E.S., DYBKJÆR, K. & PIASECKI, S. 2010. *Lithostratigraphy of the Upper Oligocene-Miocene Succession in Denmark*. Geological Survey of Denmark and Greenland Bulletin **22**, 1–92.

RASMUSSEN, E.S., VEJBÆK, O.V., BIDSTRUP, T., PIASECKI, S. & DYBKJÆR, K. 2005. Late Cenozoic depositional history of the Danish North Sea Basin: implications for the petroleum systems in the Kraka, Halfdan, Siri and Nini Fileds. *In*: DORÉ, A.G. & VINING, B.A. (eds), *Petroleum Geology of Northwest Europe and Global Prospectives*: Geological Society of London, Proceedings of the 6th Conference, 1347–1358.

SARNTHEIN, M., BARTOLI, G., PRANGE, M., SCHMITTNER, A., SCHNEIDER, B., WEINELT, M., ANDERSEN, N. & GARBE-SCHÖNBERG, D. 2009. Mid-Pliocene shifts in ocean overturning circulation and the onset of Quaternary-style climates. *Climate of the Past* **5**, 269–283.

SCHÄFER, A., UTESCHER, T., KLETT, M. & VALDIVIA-MANCHEGO, M. 2005. The Cenozoic Lower Rhine Basin – rifting, sedimentation, and cyclic stratigraphy. *International Journal of Earth Sciences/ Geologische Rundschau* **94**, 621–639.

SCHÄFER, A., UTESCHER, T. & MÖRS, T. 2004. Stratigraphy of the Cenozoic Lower Rhine Basin, northwestern Germany. *Newsletters on Stratigraphy* **40**, 73–110.

SCHNEIDER, H. & THIELE, S. 1965. *Geohydrologie des Erftgebietes*. Ministerium für Ernährung Landwirtschaft und Forsten NRW, Düsseldorf.

SHACKLETON, N.J., CROWHURST, S.J., WEEDON, G.P. & LASKAR, J. 1999. Astronomical calibration of Oligocene–Miocene times. *Philosophical Transactions of the Royal Society London: Mathematical, Physical & Engineering Sciences A* **357**, 1907–1929.

STRAUSS, C., ASHRAF, A.R. & MOSBRUGGER, V. 1993. *Marines Phytoplankton mit organischer Wandung aus mio-/pliozänen Deckschichten des Niederrheinischen Braunkohlenbeckens*. Abstract, APP Confrence, 1993, Berlin.

SUGARMAN, P.J., MCCARTAN, L., MILLER, K.G., FEIGENSON, M.D., PEKAR, S., KISTLER, R.W. & ROBINSON, A.G. 1997. Strontium isotope correlation of Oligocene to Miocene sequences, New Jersey and Florida. *In*: MILLER, K.G. & SNYDER, S.W. (eds), *Proceedings of the Ocean Drilling Program, Scientific Results* **150**, 147–159.

SYABRYAJ, S., MOLCHANOFF, S., UTESCHER, T. & BRUCH, A.A. 2007. Changes of climate and vegetation during the Miocene on the territory of Ukraine. *Palaeogeography, Palaeoclimatology, Palaeoecology* **253**, 153–168.

TURCO, E., HILGEN, F., LOURENS, L., SHACKLETON, N.J. & ZACHARIASSE, J.W. 2001. Punctuated evolution of global climate cooling during the late Middle to early late Miocene: high resolution planktonic forminiferal and oxygen isotope records from the Mediterranean. *Paleoceanography* **16**, 405–423.

UTESCHER, T., DORDJEVIC-MILUTINOVIC, D., BRUCH, A. & MOSBRUGGER, V. 2007. Palaeoclimate and vegetation change in Serbia during the last 30 Ma. *Palaeogeography, Palaeoclimatology, Palaeoecology* **253**, 157–168.

Utescher, T., Gebka, M., Mosbrugger, V., Schilling, H.-D. & Ashraf, A.R. 1997. Regional palaeontological-climatological palaeoclimate reconstruction of the Neogene Lower Rhine Embayment. Mededelingen Nederlands Instituut voor Toegepaste Geowetenschappen (TNO) **58**, 263–271.

Utescher, T. & Mosbrugger, V. 2010. *The Palaeoflora Database* (at http://www.palaeoflora.de)

Utescher, T., Mosbrugger, V. & Ashraf, A.R. 2000. Terrestrial climate evolution in Northwest Germany over the last 25 million years. *Palaios* **15**, 430–449.

Utescher, T., Mosbrugger, V., Ivanov, D. & Dilcher, D.L. 2009. Present-day climatic equivalents of European Cenozoic climates. *Earth and Planetary Science Letters* **284**, 544–552.

Van Dam, J.A. 2006. Geographic and temporal patterns in the late Neogene (12–3 Ma) aridification of Europe. The use of small mammals as paleoprecipitation proxies. *Palaeogeography, Palaeoclimatology, Palaeoecology* **238**, 190–218.

Van der Burgh, J. 1988. Some local floras from the Neogene of the Lower Rhenish Basin. *Journal of Tertiary Research* **9**, 181–212.

Van der Burgh, J. & Zetter, R. 1998. Plant mega- and microfossil assemblages from the Brunssumian of 'Hambach' near Düren, B.R.D. *Review of Palaeobotany and Palynology* **101**, 209–256.

Von der Brelie, G. 1968. Zur mikrofloristischen Schichtengliederung im rheinischen Braunkohlenrevier. *Fortschritte der Geologie Rheinland und Westfalen* **16**, 85–102.

Westerhold, T., Bickert, T. & Röhl, U. 2005. Middle to late Miocene oxygen isotope stratigraphy of ODP site 1085 (SE Atlantic): new constrains on Miocene climate variability and sea-level fluctuations. *Palaeogeography, Palaeoclimatology, Palaeoecology* **217**, 205–222.

Williams, G.L., Brinkhuis, H., Pearce, M.A, Fensome, R.A. & Weegink, J.W. 2004. Southern ocean and global dinoflagellate cyst events compared: Index events for the late Cretaceous-Neogene, 1–98. *In*: Exon, N.F., Kennet, J.P. & Malone, M.J. (eds), *Proceedings of the Ocean Drilling Program, Scientific Results* **189**.

Zachos, J.C., Dickens, G.R. & Zeebe, R.E. 2008. An early Cenozoic perspective on greenhouse warming and carbon-cycle dynamics. *Nature* **451**, 279–283.

Zachos, J.C., Pagani, M., Stone, L., Thomas, E. & Billups, K. 2001. Trends, rhythms, and aberrations in global climates 65 Ma to present. *Science* **292**, 686–293.

Zagwijn, W.H. 1989. The Netherlands during the Tertiary and the Quaternary. A case history of coastal lowland evolution. *Geologie* en Mijnbouw **68**, 107–120.

Zagwijn, W.H. & Hager, H. 1987. Correlations of continental and marine Neogene deposits in the South-Eastern Netherlands and the Lower Rhine district. *Mededelingen van de Werkgroep voor Tertiaire en Kwartaire Geologie* **24**, 59–78.